Identification of 1,5-Naphthyridine Derivatives as a Novel Series of Potent and Selective TGF-β Type I Receptor Inhibitors

Françoise Gellibert,*[,†] James Woolven,[‡] Marie-Hélène Fouchet,[†] Neil Mathews,[§,||] Helen Goodland,[||] Victoria Lovegrove,[||] Alain Laroze,[†] Van-Loc Nguyen,[†] Stéphane Sautet,[†] Ruolan Wang,[⊥] Cheryl Janson,[#,×] Ward Smith,[▽,×] Gaël Krysa,[⊗] Valérie Boullay,[⊗] Anne-Charlotte de Gouville,[⊗] Stéphane Huet,[⊗] and David Hartley[||]

Departments of Medicinal Chemistry and Biology, GlaxoSmithKline, 25-27 Avenue du Québec, 91951 Les Ulis, France, Discovery Research, Computational and Structural Science, and Department of Medicinal Chemistry, GlaxoSmithKline, Gunnels Wood Road, Stevenage, Hertfordshire SG1 2NY, United Kingdom, Discovery Research, Assay Development and Compound Profiling, GlaxoSmithKline, Five Moore Drive, P.O. Box 13398, Research Triangle Park, North Carolina 27709, and Discovery Research, GlaxoSmithKline, 709 Swedeland Road, King of Prussia, Pennsylvania 19406

Received January 30, 2004

Optimization of the screening hit **1** led to the identification of novel 1,5-naphthyridine aminothiazole and pyrazole derivatives, which are potent and selective inhibitors of the transforming growth factor-β type I receptor, ALK5. Compounds **15** and **19**, which inhibited ALK5 autophosphorylation with $IC_{50} = 6$ and 4 nM, respectively, showed potent activities in both binding and cellular assays and exhibited selectivity over p38 mitogen-activated protein kinase. The X-ray crystal structure of **19** in complex with human ALK5 is described, confirming the binding mode proposed from docking studies.

Introduction

Transforming growth factor (TGF-β) is a pluripotent cytokine involved in a variety of biological processes such as development, cell growth, differentiation, cell adhesion, migration, extracellular matrix (ECM) deposition, and immune response regulation.[1] This cytokine regulates not only the ECM deposition in response to tissue injury, thus contributing to the healing process, but is also involved in pathological fibrosis.[2] Indeed, TGF-β overexpression has been implicated in multiple disease states including pulmonary fibrosis, liver fibrosis, renal glomerulosclerosis, and cancer.[3−5] TGF-β belongs to the TGF-β superfamily, which includes in humans the three TGF-β isoforms (TGF-β1, TGF-β2, and TGF-β3), the activins, and the bone morphogenetic proteins.[6] TGF-β1 is the prototypic member of this family of cytokines that signals through a family of transmembrane serine/threonine kinase receptors. These receptors can be divided into two classes, the type I or activin like kinase (ALK) receptors and the type II receptors.[7,8] The ALK receptors are distinguished from the type II receptors in that they lack the serine/threonine rich intracellular tail, possess serine/threonine kinase domains that are homologous between type I receptors, and share a common sequence motif called the GS domain. The GS domain is at the amino terminal end of the intracellular kinase domain and is critical for activation by the type II receptor.[9] Several studies have shown that TGF-β signaling requires both the ALK and the type II receptors. Specifically, the binding of TGF-β1 to the type II receptor causes phosphorylation of the GS domain of the TGF-β type I receptor, ALK5. The ALK5 receptor, in turn, phosphorylates the cytoplasmic proteins smad2 and smad3 at two carboxyl terminal serines. The phosphorylated smad proteins form heteromeric complexes of smad2, smad3, and smad4, after which the complex translocates into the nucleus to effect gene transcription.[10]

Chart 1

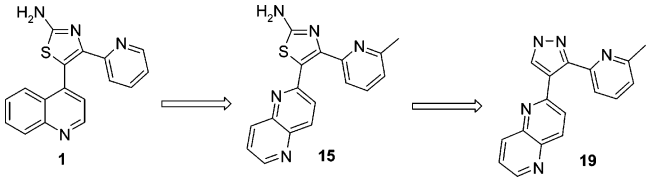

A program was initiated to identify small molecules inhibiting the TGF-β signaling pathway. High throughput screening (HTS) of our corporate compound collection was carried out using a TGF-β-dependent transcriptional assay, comprising a HepG2 cell line stably transfected with a luciferase reporter gene driven by the PAI-1 promoter. This screen identified the aminothiazole derivative **1** as a potent inhibitor of TGF-β signaling ($IC_{50} = 429$ nM). We describe below the optimization of **1** to give a series of high-affinity ALK5 inhibitors (Chart 1). A pyrazole compound **19** was cocrystallized with ALK5, and the structure of the complex was determined by X-ray crystallography.

Results and Discussion

Consideration of the structure of **1** strongly suggested that it might inhibit a kinase, and ALK5 appeared a likely candidate. Accordingly, an ALK5 autophospho-

* To whom correspondence should be addressed. Tel: +33 1 69 29 61 28. Fax: +33 1 69 07 48 92. E-mail: fjg23217@gsk.com.
† Department of Medicinal Chemistry, GlaxoSmithKline, Les Ulis.
‡ Discovery Research, Computational and Structural Science, GlaxoSmithKline.
§ Current address: Arrow Therapeutics, Britannia House, 7 Trinity St., London, SE1 1DA, U.K.
|| Department of Medicinal Chemistry, GlaxoSmithKline, Stevenage.
⊥ Discovery Research, Assay Development and Compound Profiling, GlaxoSmithKline.
Current address: Shamrock Structures, 1440 Davey Road, Woodridge, IL 60517.
▽ Current address: Argonne National Laboratory, 9700 South Cass Avenue, Argonne, IL 60439.
⊗ Department of Biology, GlaxoSmithKline, Les Ulis.
× GlaxoSmithKline, King of Prussia, PA 19406.

10.1021/jm0400247 CCC: $27.50
Published on Web 08/04/2004

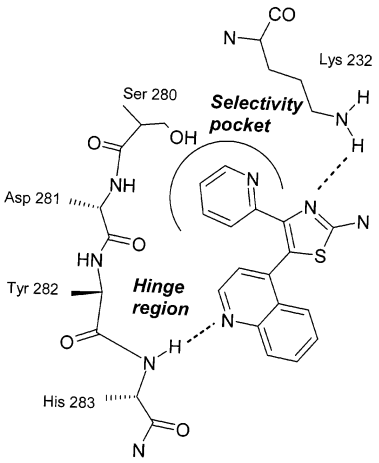

Figure 1. Schematic drawing of aminothiazole **1** potential binding mode in the ATP binding site of the ALK5−FKBP12 complex. The interactions between inhibitor and ALK5 residues are shown with dotted lines.

rylation assay was constructed using the purified human ALK5 kinase domain produced in Sf9 insect cells. Aminothiazole **1** inhibited ALK5 activity in this assay with an IC_{50} of 274 nM. While presenting some structural analogy with p38 MAP kinase inhibitors,[11] this compound did not exhibit p38 MAP kinase activity when tested in a relevant binding assay (IC_{50} > 16 μM). A chemistry program was initiated with the aim of increasing potency. To support the study of structure−activity relationships (SAR) within the series, a binding assay was set up in which the ability of the test compounds to displace a rhodamine green-labeled ligand from recombinant GST-ALK5 was measured. In this assay, **1** exhibited an IC_{50} of 724 nM. The compounds were evaluated in both the binding and the TGF-β-dependent cellular assay, and the most potent compounds were also tested in the ALK5 autophosphorylation assay. At the outset of this work, no structures of ALK5 inhibitors cocrystallized with the protein had been published. However, the crystal structure of an inactive form of ALK5 complexed to FKBP12[9] was available and this was used as a basis for docking studies.

Binding Mode Hypothesis. On the basis of the crystal structure of the ALK5−FKBP12 complex, we carried out molecular modeling studies to support the medicinal chemistry program. Knowing that compound **1** inhibited ALK5 by occupation of the ATP binding site, the binding was ATP competitive (data not shown), and comparison of ALK5 with a range of other kinase−inhibitor complexes for which structural information was available enabled us to characterize residues that could interact with the ligand. Subsequent docking studies were performed to identify a potential binding mode of compound **1** (Figure 1).

In the preferred model, the quinoline moiety interacts with the backbone of amino acids (residues 281−283) that links the N- and C-terminal domains of the kinase (hinge region), a region normally occupied by the adenine ring of ATP. The main hydrogen bond in this region links quinoline N1 and the backbone NH of His-283. An analogous hydrogen bond acceptor−donor pair occurs in all inhibitor−kinase crystal structures and is also seen for N1 of adenine in ATP.

The N3 of the aminothiazole scaffold may interact with the side chain of Lys-232. This amino acid is included in the catalytic segment, and an equivalent hydrogen bond had previously been seen between p38 MAP kinase inhibitors and Lys-53.[12] As Lys-53 is a highly conserved residue in the ATP binding site, this interaction is unlikely to contribute to selectivity.

The pyridyl moiety is directed into the interior of the protein toward Ser-280 in the so-called "selectivity pocket", as established for p38 MAP kinase.[13] This selectivity pocket is behind and orthogonal to the adenine binding site and is not utilized by ATP. Ser-280 may be the key protein feature involved in inhibitor selectivity and is equivalent to Thr-106, the so-called "gate keeper" residue in p38 MAP kinase.[12] These are the main residues governing the size and accessibility of the selectivity pocket. Only a limited number of kinases have threonine or serine as gate keeper residues, most having larger residues at this position, which are believed to block the formation of the pocket.

SARs. In an attempt to increase the potency of this novel series of ALK5 inhibitors, the three heterocyclic subunits were modified in turn. To explore the selectivity pocket toward which the pyridin-2-yl is directed, the pyridine moiety was replaced by other aromatic groups (Table 1). The pyridin-3-yl analogue **2** showed a decrease in binding affinity, suggesting that the nitrogen atom of the 2-pyridyl ring might be involved in a hydrogen bonding interaction with the protein, even though this was not evident from the docking studies. In support of this supposition, the thiazol-2-yl compound **3** retained the potency of **1** in the binding assay. However, the 2-fluorophenyl analogue **4** also showed a similar level of binding affinity, so, clearly, an appropriately positioned nitrogen atom is not necessary for activity, although it remains possible that the 2-fluorophenyl group could participate in hydrogen bonding. Replacement of the 2-fluoro substituent by a 2-methoxy group **5** abolished the binding to ALK5. It was apparent from the docking studies that the pyridin-2-yl of **1** and the Ser-280 oxygen of the protein were in close proximity, with a distance of 3.21 Å measured between the pyridine centroid and the Ser-280 oxygen. This was suggestive of a possible electrostatic interaction, consistent with the observed activity of the 2-fluorophenyl analogue **4**. To explore this idea further, the pyridin-2-yl ring was substituted with electron-withdrawing and -donating groups, some representatives of which are shown in Table 1. The electron deficient 5-chloro (**6**) and 4-chloro (**7**) analogues retained the binding affinity to ALK5, whereas the electron-rich 5-methyl derivative (**8**) showed a significantly decreased affinity. These results partly support the hypothesis that an unfavorable electrostatic interaction between the pyridine ring and the Ser-280 hydroxyl is exacerbated when the pyridine bears an electron-donating group as in **8**, although, if this is the case, it is not clear why the electron deficient analogues **6** and **7** do not show enhanced affinity. The above compounds were tested in the TGF-β cellular assay, and all showed decreased potency, so it appeared that the 2-pyridyl core was important for cellular activity.

Accordingly, the pyridin-2-yl group was retained while modifications were made to the quinoline region of the series (Table 2). Replacement of the quinoline by a

Table 1. Replacement of the Pyridyl Moiety

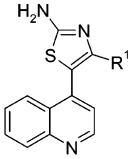

5-(4-Quinolinyl)-1,3-thiazol-2-amine derivatives **1, 8**

Compd	R^1	ALK5 Binding IC50 (μM)[a]	TGF-β• cellular assay IC50 (μM)[b]
1		0.724 (0.095-5.521)	0.429±0.173
2		3.981(2.423-6.540)	>10
3		1.175 (0.783-1.764)	6.589±1.388
4		1.259 (0.356-4.455)	6.67±1.009
5		>10	>10
6	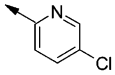	1.778 (0.864-3.661)	>10
7	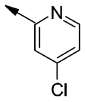	1.023 (0.289-3.621)	>10
8	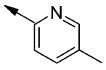	>10	>10

[a] Values are the means of two or more separate experiments; pIC_{50} values were calculated, and the mean pIC_{50} was converted to IC_{50}. The numbers in parentheses are the 95% confidence limits on the pIC_{50} converted to IC_{50} values and reported as the limits of the IC_{50}. [b] Mean values ± SD for a minimum of three determinations.

Table 2. Replacement of the Quinoline Group

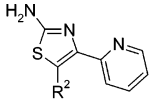

4-(2-Pyridinyl)-1,3-thiazol-2-amine derivatives **9, 14a-b**

Compd	R^{2a}	ALK5 binding IC50 (μM)[b]	TGF-β cellular assay IC50 (μM)[c]
9	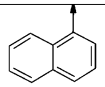	10.965 (5.326-22.574)	>10
10	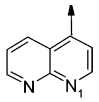	7.943 (3.221-19.588)	>10
11	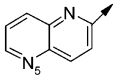	0.040 (0.038-0.042)	0.126±0.073
12	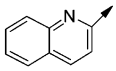	3.548 (1.375-9.154)	>10
13	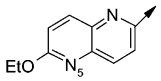	>10	>10
14a	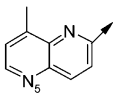	0.030 (0.021-0.042)	0.223±0.141
14b	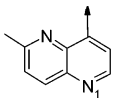	0.380 (0.180-0.790)	0.268±0.093

[a] Labeled nitrogen is involved in an H-bond interaction with His283. [b] Values are the means of two or more separate experiments; pIC_{50} values were calculated, and the mean pIC_{50} was converted to IC_{50}. The numbers in parentheses are the 95% confidence limits on the pIC_{50} converted to IC_{50} values and reported as the limits of the IC_{50}. [c] Mean values ± SD for a minimum of two determinations.

naphthalene nucleus **9** abolished the binding to ALK5, supporting the hypothesis that the nitrogen atom of the quinoline **1** was engaged in an important interaction with the protein. Evaluation of a range of alternative heterocyclic systems using docking studies suggested that the naphthyridine system might be an appropriate replacement for the quinoline. In particular, two templates were selected based on their potential hydrogen bond interaction with the backbone NH of His-283. While incorporation of the 1,8-naphthyridine nucleus **10** was detrimental for binding to ALK5, the 1,5-naphthyridine **11** showed a 10-fold increase in binding potency as compared to **1**. For the 1,8-naphthyridine **10**, docking studies showed a good overlay with the quinoline **1**. The distance between the N1 nitrogen of the 1,8-naphthyridine core and the backbone NH of His-283 was 2.74 Å, consistent with the desired H-bonding interaction. However, the close proximity of the N8 nitrogen and the backbone carbonyl of His-283 (distance of 3.82 Å) may be indicative of a repulsive interaction as compared with the quinoline **1**, which might account for the loss in potency. On the other hand, two parameters might explain the gain in potency for the 1,5-naphthyridine **11**. First, the hydrogen bond interaction with the backbone NH of His-283 was maintained despite a shift of 1.13 Å for naphthyridine N5 as compared to quinoline N1. Second, the naphthyridine nucleus was more deeply embedded in the hinge region as compared to the quinoline, as illustrated in Figure 2.

The quinolin-2-yl analogue **12** showed a 70-fold reduced binding affinity as compared to **11**, demonstrating that the N5 nitrogen was key for optimal binding affinity. To explore the hinge region, which accommodates the naphthyridine nucleus, substitution at positions C6 and C8 was carried out. The C6-ethoxy analogue **13** showed a decreased binding affinity, whereas the C8-methyl analogue **14a** retained ALK5 inhibitory potency (Table 2). The loss of potency on substitution at C6 can be explained by the location of the naphthyridine nucleus in a deep well-defined pocket of restricted size. Docking studies suggest an unfavorable interaction between the C6-substituent and the backbone carbonyl of Asp-281. The C8-methyl group of compound **14a**, on the other hand, is directed toward the opening of the active site (Figure 2), so it is not surprising that this compound retained binding affinity. Interestingly, the

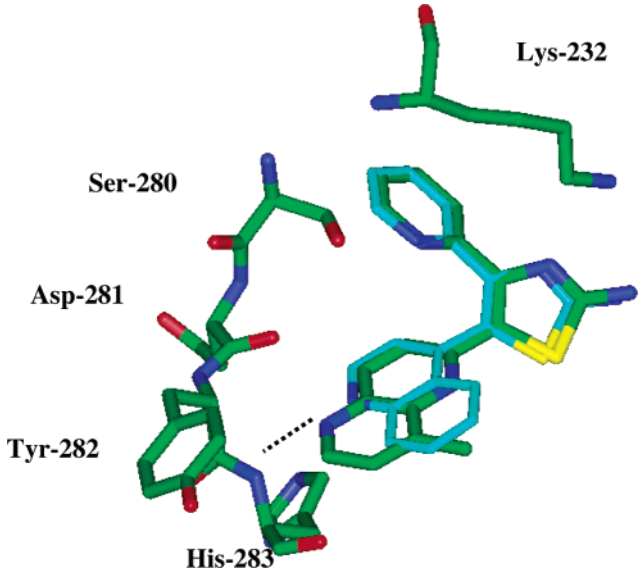

Figure 2. Overlay of 1,5-naphthyridine **14a** (green) and quinoline derivative **1** (cyan) docked in the ALK5−FKBP12 complex. The interaction between N5 and His-283 is shown with dotted line.

1,5-naphthyridin-4-yl analogue **14b** presented a binding affinity comparable to **1**. In this case, this is the N1 nitrogen of the 1,5-naphthyridine group that is involved in the hydrogen bond interaction with the backbone NH of His-283.

Compounds **11** and **14a**,**b** were more potent than **1** in the TGF-β cellular assay. Compound **11** was also a potent inhibitor of ALK5 autophosphorylation (IC_{50} = 20 nM), exhibiting a 10-fold higher potency than **1**. On the basis of these encouraging results, further modifications were made to the pyridin-2-yl moiety, this time retaining the 1,5-naphthyridine core (Table 3). Introduction of a methyl at the C6-position led to an equipotent ALK5 inhibitor **15** with also a 6-fold increase in potency in the TGF-β cellular assay. Replacement of the pyridin-2-yl ring with 4-fluorophenyl **16** or 3-chlorophenyl **17** retained the in vitro potency, showing that the selectivity pocket is able to accommodate small lipophilic groups such as methyl or chlorine. Although the binding affinity was maintained for the phenyl derivatives **16** and **17**, this structural modification had an impact on selectivity vs p38 MAP kinase. Indeed, both compounds **16** and **17** exhibited significant binding affinity for p38 as compared to the pyridin-2-yl derivatives **11** and **15**.

To identify potent ALK5 inhibitors, we investigated other chemical series in parallel of this work, exploring the replacement of the central core by different heterocycles. We previously identified the pyrazole[14] as an interesting scaffold to replace the aminothiazole core and decided to combine this modification with the 1,5-naphthyridine template. More recently, pyrazole compounds were also described in the literature[15] as potent ALK5 inhibitors. Both pyrazoles **18** and **19** showed similar enzyme inhibitory potencies to the corresponding aminothiazole analogues **11** and **15** with no loss in selectivity vs p38 MAP kinase (Table 4). This would appear to suggest that the ring nitrogen atom of the aminothiazole is more important for ALK5 inhibitory activity than the extracyclic amino group. Both pyrazoles presented cellular potency comparable to that obtained for the corresponding aminothiazoles.

In addition, compound **19** was tested against a panel of kinases (Table 5) and did not present any inhibitory activity at 16 μM on these kinases.

Binding Mode Description of Compound 19 in ALK5 from X-ray Crystal Structure. To determine with precision the binding mode and validate our previous hypotheses, a representative example of the naphthyridine series, compound **19**, was cocrystallized with ALK5. The RMS deviation (backbone atoms) of the ALK5−FKBP12 complex active site is 1.14 Å from the ALK5−**19** crystal structure active site indicating that the docking studies based on the ALK5−FKBP12 complex were indeed relevant to support the medicinal chemistry program. The main interactions suggested by the model were shown to be valid following examination of the cocrystallization structure. Moreover, additional structural characteristics, particularly in the selectivity pocket, shed interesting light on the SAR data as shown in Figure 3.

Compound **19** binds in the ATP site with the 1,5-naphthyridine N5 interacting with the backbone NH of His-283. Pyrazoles N1 and N2 are involved in hydrogen bonds with the side chains of Asp-351 and Lys-232,

Table 3. 1,5-Naphthyridine Aminothiazoles

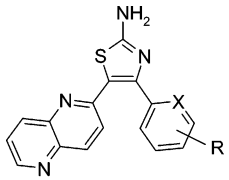

11, 15-17

compd	X	R	ALK5 binding IC_{50} (μM)[a]	ALK5 auto-P IC_{50} (μM)[b]	TGF-β cellular assay IC_{50} (μM)[b]	p38 MAPK inhibition[c] IC_{50} (μM)[d]
11	N	H	0.040 (0.038−0.042)	0.020 ± 0.004	0.126 ± 0.073	>16
15	N	6-CH3	0.025 (0.019−0.032)	0.006 ± 0.002	0.016 ± 0.001	>16
16	CH	4-F	0.042 (0.040−0.044)	0.011 ± 0.004	0.032 ± 0.009	0.490 (0.208−1.155)
17	CH	3-Cl	0.023 (0.020−0.026)	0.013 ± 0.004	0.016 ± 0.005	0.363 (0.242−0.545)

[a] Values are the means of two or more separate experiments; pIC_{50} values were calculated, and the mean pIC_{50} was converted to IC_{50}. The numbers in parentheses are the 95% confidence limits on the pIC_{50} converted to IC_{50} values and reported as the limits of the IC_{50}. [b] Mean values ± SD for a minimum of two determinations. [c] Inhibition of binding to p38. [d] Mean values on three separate experiments performed in a fluorescence polarization assay mode where displacement of fluorescently labeled ATP competitive inhibitor[24] by different concentrations of compound was used to calculate a binding IC_{50}. The numbers in parentheses are the 95% confidence limits on the pIC_{50} converted to IC_{50} values and reported as the limits of the IC_{50}.

Table 4. Pyrazole Compounds

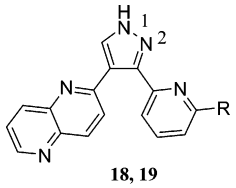

18, 19

compd	R	ALK5 binding IC$_{50}$ (μM)[a]	ALK5 auto-P IC$_{50}$ (μM)[b]	TGF-β cellular assay IC$_{50}$ (μM)[b]	p38 MAPK inhibition[c] IC$_{50}$ (μM)
18	H	0.030 (0.029−0.032)	0.019 ± 0.005	0.054 ± 0.001	>16
19	CH_3	0.023 (0.020−0.026)	0.004 ± 0.001	0.018 ± 0.006	>16

[a] Values are the means of two or more separate experiments, and the 95% confidence limits on the pIC$_{50}$ are converted to IC$_{50}$ values and reported as the limits of the IC$_{50}$. [b] Values are the means of two or more separate experiments ± SD. [c] Inhibition of binding to p38. Experiments were duplicated and performed in a fluorescence polarization assay mode where displacement of fluorescently labeled ATP competitive inhibitor[24] by different concentrations of compound **19** was used to calculate a binding IC$_{50}$.

Table 5. Selectivity of Compound **19** against a Panel of Kinases[a]

compd	p38 MAPK IC$_{50}$ (μM)[b]	LCK(murine) IC$_{50}$ (μM)[c]	JNK1 IC$_{50}$ (μM)[b]	JNK3 IC$_{50}$ (μM)[c]	ITK IC$_{50}$ (μM)[c]	MSK1 IC$_{50}$ (μM)[b]	GSK3 IC$_{50}$ (μM)[b]	MLK3 IC$_{50}$ (μM)[b]	B-RAF IC$_{50}$ (μM)[b]
19	>16	>16	>16	>16	>16	>16	>16	>16	>16

[a] All enzymes are human unless stated otherwise. [b] Inhibition of binding to kinase. All tests were duplicated and performed in a fluorescence polarization assay mode. [c] Inhibition of kinase activity. All tests were duplicated and performed in an HTRF assay mode where phosphorylation of a biotinylated specific peptide is measured using europium-labeled antibodies rised against phospho-peptide and streptavidin-labeled APC.

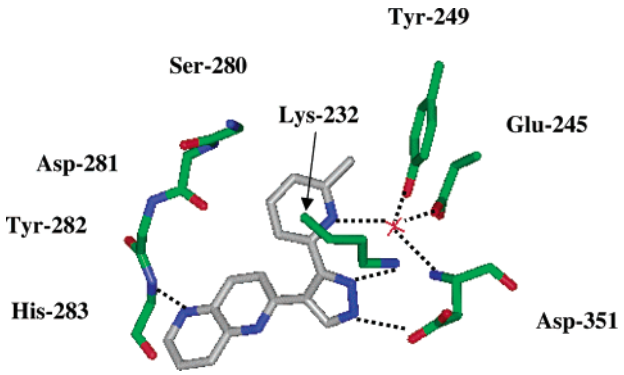

Figure 3. X-ray crystal structure of 1,5-naphthyridine compound **19** bound to the ATP binding site of the kinase domain of human ALK-5. The interactions less than 3.1 Å are highlighted with black dotted lines.

respectively. In the X-ray crystal structure that was described by workers at Lilly for 4-[3-(pyridin-2-yl)-1*H*-pyrazol-4-yl]quinoline,[15] the N1−Asp-351 hydrogen bond was not mentioned, while it was recently observed by another team for the same compound.[16] As was suggested by Sawyer et al.,[15] the flexibility of the Asp-351 side chain might play a key role in the ability of ALK5 to accommodate a range of inhibitors displaying a variety of steric profiles in the hinge region.

Pyridine N1 forms a hydrogen bond to a water molecule that also interacts with side chains of Tyr-249, Glu-245, and the backbone of Asp-351. This pyridine N1−H_2O hydrogen bond may explain why a hydrogen bond acceptor group in this position is beneficial, as noted above. This water molecule, although located deep inside the active site, is surrounded by a polar environment, which may stabilize it (Figure 4). An analogous water molecule was observed in the crystal structures of aryl-substituted pyrazole ALK5 inhibitors[15] but was not detected in the ALK5−FKBP12 complex. This may suggest that it is brought into the active site with the solvated ligand. Determination of a crystal structure of an inhibitor without this hydrogen bond capability (for example compound **16** or **17**) would help to test this hypothesis.

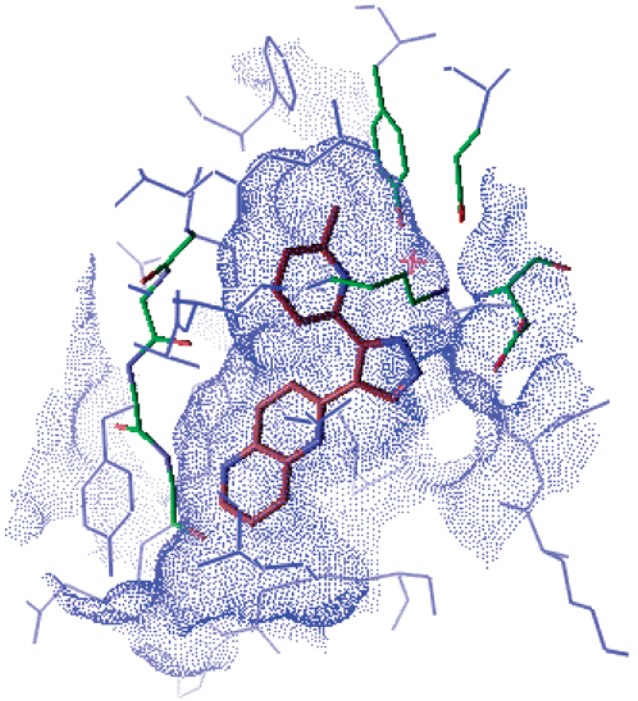

Figure 4. X-ray crystal structure of 1,5-naphthyridine compound **19** complexed with human ALK5. The molecular surface of the ATP binding site is represented by blue dots. The water molecule is indicated in red, and key amino acids for interactions are represented in green.

Apart from this pyridine N1−H_2O interaction, the ligand is not involved in other hydrogen bonds within this region. The 6-methyl substituent is located in a small, mainly hydrophobic, pocket (Figure 4). The pyridine ring is close to and parallel with the side chain of the Ser-280 (3.27 Å between the pyridine centroid and the oxygen of Ser-280). An overlay of crystal structures

Scheme 1[a]

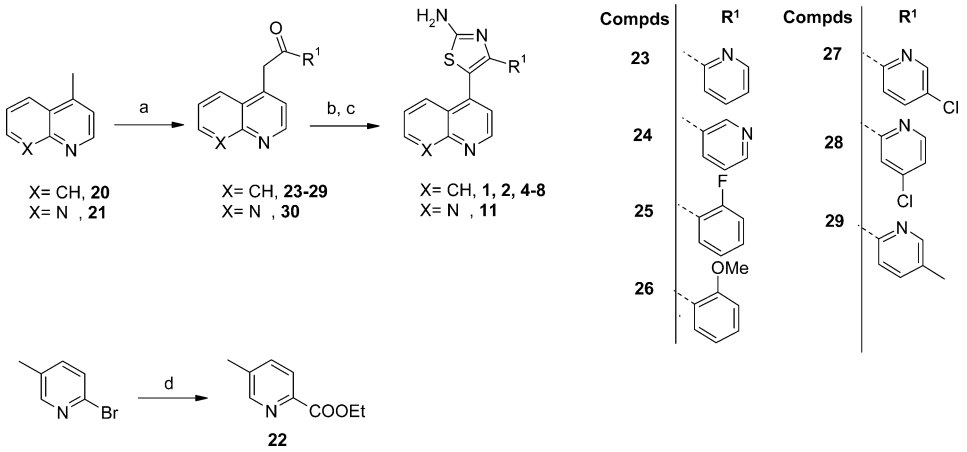

[a] Reagents and conditions: (a) R^1COOEt, KHMDS, THF, −50°C. (b) Polymer-supported pyridinium perbromide, THF, room temperature. (c) Thiourea, EtOH, reflux. (d) CO(atm), $Pd(OAc)_2$, dppp, TEA, EtOH, DMF, 80 °C.

of p38 and ALK5 shows that the hydroxyl side chain of Ser-280 is superposed on the methyl of Thr-106 but not its hydroxyl. As a consequence, the nature of the interaction with the inhibitor will be different between enzymes and this may explain the selectivity of this type of ALK5 inhibitor vs p38 MAP kinase. Two types of interactions seem to coexist in the region: the hydrogen bond with N1 of the pyridyl and an electronic interaction between the O of Ser-280 and the ring of the ligand. This may explain the SAR showing that either a pyridine or a phenyl, substituted with small electron-withdrawing groups, is necessary to optimize the interaction.

Chemistry

The quinolin-4-yl aminothiazole derivatives were prepared according to the general method described in Scheme 1. Lepidine **20** was condensed with the corresponding esters (R^1COOEt) in the presence of potassium bis(trimethylsilyl)amide in anhydrous THF in a range of temperatures between −50 and −78 °C to give the ketones **23**−**29**. The 2-carbethoxy-5-methylpyridine **22** was prepared by carboethoxylation[17] of 2-bromo-5-methylpyridine in the presence of a catalytic amount of palladium acetate and 1,3-bis(diphenylphosphino)-propane (dppp) in a mixture of triethylamine/ethanol under a CO atmosphere. Subsequent bromination of the ketones **23**−**29** with bromine or polymer-supported pyridinium perbromide afforded the corresponding α-bromoketones, which were immediately reacted with thiourea to provide the aminothiazole compounds **1**, **2**, and **4**−**8**. The same synthetic pathway was used for the preparation of the 1,8-naphthyridine **11** starting from 4-methyl[1,8]naphthyridine **21** (Scheme 1). The 4-methyl-[1,8]naphthyridine was prepared in a one step synthesis applying the Skraup reaction to the commercially available 2-amino-4-methylpyridine as described in the literature.[18]

Another approach was followed for the preparation of compound **3** (Scheme 2). The commercially available 2-acetylthiazole was condensed with 4-chloroquinoline in the presence of sodium hydride to afford the ketone **31**. Bromination and reaction with thiourea using the conditions previously described afforded the aminothiazole **3**.

Scheme 2[a]

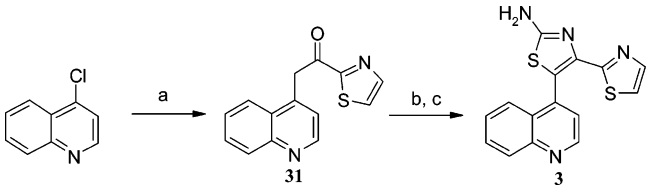

[a] Reagents and conditions: (a) 2-Acetylthiazole, NaH, THF, 0 °C to room temperature. (b) Polymer-supported pyridinium perbromide, THF, room temperature. (c) Thiourea, EtOH, reflux.

Scheme 3[a]

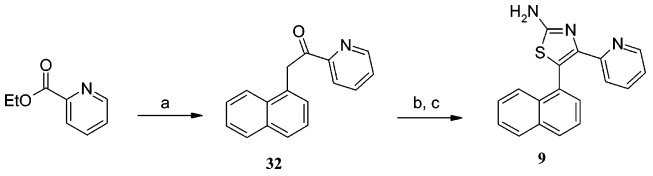

[a] Reagents and conditions: (a) 1-(Chloromethyl)naphthalene, Mg, Et_2O, reflux. (b) Polymer-supported pyridinium perbromide, THF, room temperature. (c) Thiourea, EtOH, reflux.

Alternatively, the ketone **32** was prepared by condensation of (1-naphthalenylmethyl) magnesium chloride with ethyl picolinate. This ketone was therefore reacted with bromine followed by thiourea to afford the naphthalene derivative **9** (Scheme 3).

The 1,5-naphthyridine derivatives **11** and **13**−**19** and the quinoline **12** were prepared following the general pathway outlined in Scheme 4. The aminothiazoles **11** and **15** and the corresponding pyrazoles **18** and **19** were accessible from common ketone intermediates. The 1,5-naphthyridines **36**−**39** were condensed with the commercially available esters of general formula (**I**) to give the corresponding ketones **41**−**46**. Subsequent bromination followed by reaction with thiourea afforded the aminothiazoles **11** and **13**−**17**. The same synthetic pathway was applied to 2-methylquinoline to give, from intermediate **47**, the aminothiazole **12**. On the other hand, treatment of the ketones **41** and **44** with *N*,*N*-dimethylformamide dimethyl acetal (DMF·DMA) in the presence of acetic acid in DMF, followed by reaction with hydrazine monohydrate, provided the pyrazoles **18** and **19**.

The 1,5-naphthyridine derivatives **36**−**39** were prepared from the commercially available 3-aminopyridine

Scheme 4[a]

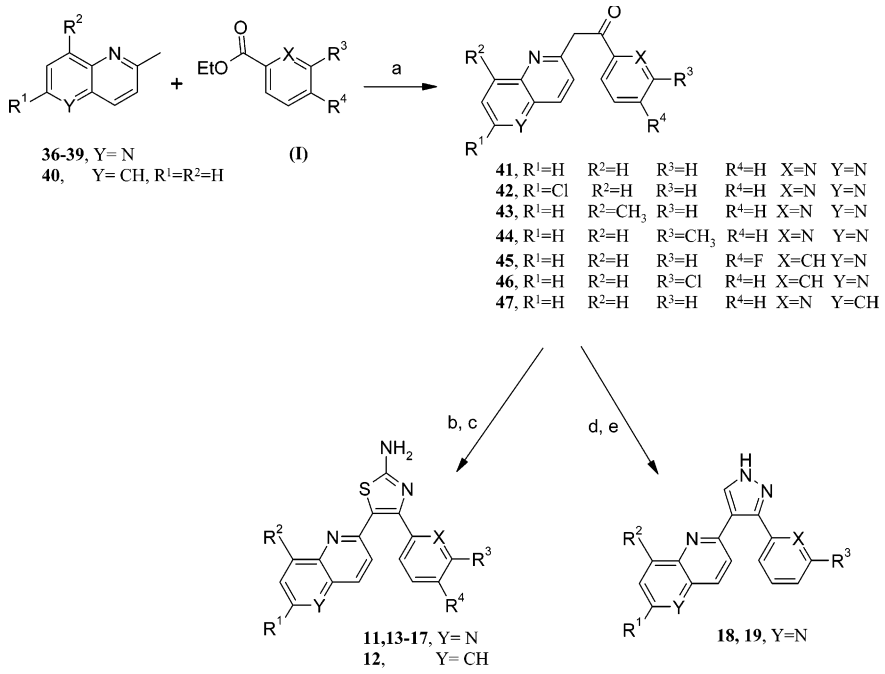

[a] Reagents and conditions: (a) KHMDS, THF, −78 °C. (b) Br_2, dioxane, room temperature or polymer-supported pyridinium perbromide, THF, room temperature. (c) Thiourea, EtOH, 78 °C. (d) DMF·DMA, acetic acid, DMF, room temperature; $N_2H_4 \cdot H_20$, DMF, room temperature.

Scheme 5[a]

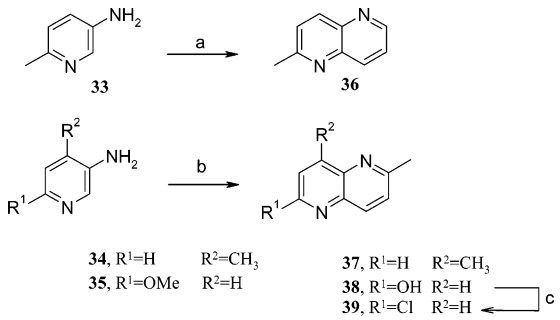

[a] Reagents and conditions: (a) Glycerol, H_2SO_4 concentrated, sodium *m*-nitrobenzenesulfonate, H_3BO_3, $FeSO_4 \cdot 7H_2O$. (b) Acetaldehyde, HCl concentrated, 0 °C. (c) $POCl_3$, reflux.

Scheme 6

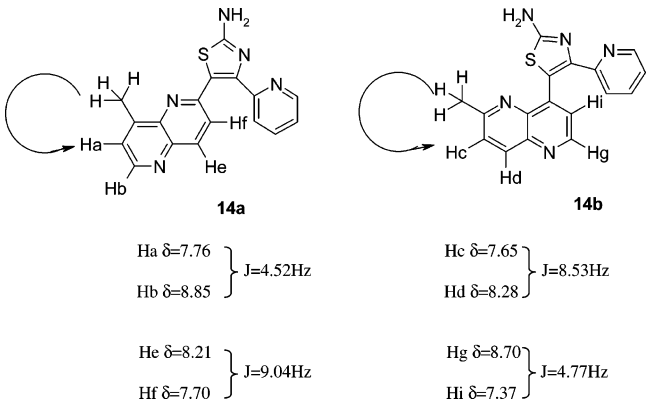

derivatives as described in Scheme 5. The 3-amino-6-picoline **33** was readily converted to the known 2-methyl-[1,5]naphthyridine **36** via a Skraup reaction,[19] whereas the 3-amino-4-methylpyridine **34** was reacted with acetaldehyde to afford the 2,8-dimethyl[1,5]naphthyridine **37**. The 2-hydroxy-6-methyl[1,5]naphthyridine **38** was obtained in the same fashion starting from 6-methoxy-3-aminopyridine **35** and was next converted to the 2-chloro-6-methyl[1,5]naphthyridine **39** with $POCl_3$.

In the case where the 2,8-dimethyl[1,5]naphthyridine **37** was condensed with ethyl picolinate, a mixture of two isomers, 2-(6-methyl-1,5-naphthyridin-4-yl)-1-(pyridin-2-yl)ethanone and 2-(8-methyl-1,5-naphthyridin-2-yl)-1-(pyridin-2-yl)ethanone, was formed and used directly in the next steps without purification. The separation of isomers was performed by chomatography on the final products **14a**,**b**, after cyclization with thiourea. The structures of compounds **14a**,**b** were assigned from NOE experiments based on the difference of the chemical shifts and ^3J couplings of their respective Hb and Hd protons (Scheme 6). The small coupling between Ha and Hb in compound **14a** (respectively between Hg and Hi in **14b**) and the large coupling between He and Hf in compound **14a** (respectively between Hc and Hd in **14b**) are characteristic for 1,5-naphthyridines. Irradiation of the methyl group for compound **14a** at δ 2.50 gave an enhancement of the proton Ha at δ 7.76, which is coupled with Hb at δ 8.85 (^3J = 4.52 Hz), while irradiation of the methyl group for compound **14b** at δ 2.54 gave an enhancement of the proton Hc at δ 7.65, which was coupled with Hd δ 8.28, with a large coupling (^3J = 8.53 Hz).

Conclusion

Two novel series of ALK5 inhibitors were identified starting from a HTS based on a TGF-β-dependent transcriptional HepG2 cellular assay. 1,5-Naphthyridin-4-yl-substituted aminothiazoles and pyrazoles showed potent inhibition of ALK5 on both the enzyme and the TGF-β-dependent cellular assays. Moreover, the pyridin-2-yl derivatives **11**, **15**, **18**, and **19** exhibited selectivity against p38 MAP kinase. The X-ray crystal structure

obtained for **19** complexed with ALK5 validated the binding mode hypothesis, which had been used to support the medicinal chemistry program. These 1,5-naphthyridine compounds show high in vitro potency and good selectivity over p38 MAP kinase and thus represent attractive tools to explore the potential benefit of ALK5 inhibition in diseases where detrimental effects of TGF-β have been described.

Experimental Section

All starting materials were commercially available and used without further purification. All reactions were carried out with the use of standard techniques under an inert atmosphere (Ar or N_2). Organic extracts were routinely dried over anhydrous sodium sulfate. Solvent removal refers to rotary evaporation under reduced pressure at 30−40 °C. The analytical thin-layer chromatography (TLC) was carried out on E. Merck 60-F_{254} precoated silica gel plates, and components were usually visualized using UV light, iodine vapor, or Dragendorff preparation. Flash column chromatography was performed using silica gel, Merck grade 60 (230−400 mesh). Melting points were determined on a hot-stage Kofler apparatus and are uncorrected. Proton NMR (^{1}H NMR) spectra were recorded at ambient temperature on Bruker Avance 250 AC, 300 DPX, or 400 DPX spectrometers using tetramethylsilane as internal standard, and proton chemical shifts are expressed in ppm in the indicated solvent. The following abbreviations are used for multiplicity of NMR signals: s = singlet, d = doublet, t = triplet, q = quadruplet, dd = double doublet, m = multiplet, dd = doublet of doublet, ddd = doublet of doublet of doublet, and bs = broad singlet. The mass spectra (MS) were recorded on a Helwett-Packard 5973 or micromass Platform-LC mass spectrometer using different techniques, including atmospheric pressure chemical ionization (APCI) or electrospray ionization (ESI). Analytical HPLC (system A) was conducted on a Chromolith Performance RP 18 column (100 mm × 4.6 mm id) eluting with 0.01 M ammonium acetate in water and 100% acetonitrile (CH_3CN), using the following elution gradient: 0−100% CH_3CN over 4 min, 100% CH_3CN over 1 min at 5 mL/min. High-resolution mass spectra were determined on a micromass LCT. Analytical HPLC (system B) was conducted on a Uptisphere-hsc column (3 μm, 33 mm × 3 mm id) eluting with 0.01 M ammonium acetate in water and 100% acetonitrile (CH_3CN) using the following elution gradient 0−5% CH_3CN over 0.5 min, gradient 5−100% CH_3CN over 3.25 min, and 100% CH_3CN over 0.75 min. For compound **9**, HPLC analysis was carried on a Agilent 1100 Series LC/MSD. Analytical HPLC (system C) was conducted using a Xterra MS C18 column (4.6 mm × 50 mm i.d) eluting with a mixture of water and acetonitrile (CH_3CN) using the following elution gradient 5−100% CH_3CN over 15 min at 1.8 mL/min. The purity of the compounds was determined on two analytic HPLC systems by UV detection. The following compounds were prepared according to literature procedures: methyl 4-chloropicolinate[20] and methyl 5-chloropicolinate.[21]

Ethyl 5-Methylpyridine-2-carboxylate (22). To a solution of 2-bromo-5-methylpyridine (10 g, 58.14 mmol) in DMF (100 mL) were added triethylamine (20.6 mL, 145 mmol), Pd $(OAc)_2$ (1.31 g, 5.81 mmol), dppp (2.4 g, 5.81 mmol), and EtOH (34.56 mL). This mixture was reacted with CO at atmospheric pressure and heated at 80 °C for 48 h. The reaction mixture was concentrated and partitioned between EtOAc and brine. The combined organic layers were dried over sodium sulfate and evaporated. The crude product was purified by flash column chromatography on silica gel eluting with cyclohexane/EtOAc 4/1 to afford **22** as a colorless oil (6.09 g, 64%). ^{1}H NMR (400 MHz, $CDCl_3$): δ 8.57 (bs, 1H), 8.03 (d, J = 8.04 Hz, 1H), 7.62 (bd, J = 8.04 Hz, 1H), 4.47 (q, J = 7.03 Hz, 2H), 2.41 (s, 3H), 1.43 (t, J = 7.03 Hz, 3H). MS (ES) m/z 165 $(M + H)^+$.

1-(Pyridin-2-yl)-2-(quinolin-4-yl)ethanone (23). To a solution of lepidine (**20**, 9.54 g, 66.63 mmol) in dry THF (100 mL) at −50 °C under argon, a solution of potassium bis-(trimethylsilyl)amide (0.5 M in toluene, 147 mL, 1.1 equiv) was added dropwise. The solution was stirred at −50 °C for 30 min, and then, a solution of ethyl picolinate (11.04 g, 73.29 mmol) in dry THF (60 mL) was added, and the reaction mixture was allowed to warm to room temperature overnight. The solvent was concentrated under reduced pressure, and the solid was precipitated with diethyl ether. The brown solid obtained was taken up into saturated NH_4Cl solution, and the aqueous phase was extracted with EtOAc. The organic layer was dried over sodium sulfate and concentrated to give **23** as an orange oil (12.83 g, 77.6%). ^{1}H NMR (250 MHz, $CDCl_3$): δ 8.78 (d, J = 4.58 Hz, 1H), 8.69 (brd, J = 4.88 Hz, 1H), 8.06 (d, J = 8.24 Hz, 1H), 7.98 (d, J = 7.94 Hz, 1H), 7.93 (d, J = 8.55 Hz, 1H), 7.79 (ddd, J = 7.94, 7.63, 1.83 Hz, 1H), 7.63 (ddd, J = 8.24, 6.71, 1.22 Hz, 1H), 7.50−7.41 (m, 2H), 7.32 (d, J = 4.27 Hz, 1H), 4.96 (s, 2H). MS (APCI) m/z 249 $(M + H)^+$.

1-(Pyridin-3-yl)-2-(quinolin-4-yl)ethanone (24). This was prepared in a manner similar to **23** from lepidine and ethyl nicotinate. ^{1}H NMR (250 MHz, $CDCl_3$): δ 9.10 (d, J = 4.5 Hz, 1H), 8.75−8.65 (m, 2H), 8.18−8.10 (m, 1H), 8.02 (d, J = 8.3 Hz, 1H), 7.70 (d, J = 8.3 Hz, 1H), 7.65−7.58 (m, 1H), 7.45−7.37 (m, 1H), 7.35−7.27 (m, 1H), 7.18−7.08 (m, 1H), 4.06 (s, 2H). MS (ES) m/z 249 $(M + H)^+$.

1-(2-Fluorophenyl)-2-(quinolin-4-yl)ethanone (25). This was prepared in a manner similar to **23** from lepidine and ethyl 2-fluorobenzoate. ^{1}H NMR (250 MHz, $CDCl_3$): δ 8.80 (d, J = 4.58 Hz, 1H), 8.09 (d, J = 8.24 Hz, 1H), 7.88−7.75 (m, 2H), 7.67 (dd, 8.24, 8.24 Hz, 1H), 7.57−7.44 (m, 2H), 7.24 (d, J = 4.58 Hz, 1H), 7.21−7.08 (m, 2H), 4.70 (s, 2H). MS (API) m/z 266 $(M + H)^+$.

1-(2-Methoxyphenyl)-2-(quinolin-4-yl)ethanone (26). This was prepared in a manner similar to **23** from lepidine and ethyl 2-(methyloxy)benzoate. ^{1}H NMR (250 MHz, $CDCl_3$): δ 8.77(d, J = 4.27 Hz, 1H), 8.06 (d, J = 8.54 Hz, 1H), 7.84 (d, J = 8.54 Hz, 1H), 7.70−7.60 (m, 2H), 7.50−7.40 (m, 2H), 7.19 (d, J = 4.58 Hz, 1H), 7.00−6.90 (m, 2H), 4.70 (s, 2H), 3.84 (3H, s). MS (API) m/z 278 $(M + H)^+$.

1-(5-Chloro-pyridin-2-yl)-2-(quinolin-4-yl)ethanone (27). This was prepared in a manner similar to **23** from lepidine and methyl 5-chloropicolinate.[16] ^{1}H NMR (400 MHz, $CDCl_3$): δ 8.87 (d, J = 4.54 Hz, 1H), 8.71 (d, J = 2.51 Hz, 1H), 8.13 (d, J = 8.54 Hz, 1H), 8.03 (d, J = 8.54 Hz, 1H), 7.99 (bd, J = 9.04 Hz, 1H,), 7.84 (dd, J = 8.54, 2.51 Hz, 1H), 7.74−7.69 (m, 1H), 7.58−7.52 (m, 1H), 7.40 (d, J = 4.02 Hz, 1H), 4.99 (s, 2H). MS (ES) m/z 283 $(M + H)^+$.

1-(4-Chloro-pyridin-2-yl)-2-(quinolin-4-yl)ethanone (28). This was prepared in a manner similar to **23** from lepidine and methyl 4-chloropicolinate.[17] ^{1}H NMR (400 MHz, $CDCl_3$): δ 8.87(d, J = 4.02 Hz, 1H), 8.68 (d, J = 5.52 Hz, 1H), 8.13 (d, J = 8.53 Hz, 1H), 8.05 (d, J = 2.00 Hz, 1H), 7.98 (bd, J = 8.53 Hz, 1H), 7.70−7.65 (m, 1H), 7.59−7.52 (m, 2H), 7.29 (d, J = 4.52 Hz, 1H), 5.01 (s, 2H).

1-(5-Methyl-pyridin-2-yl)-2-(quinolin-4-yl)ethanone (29). This was prepared in a manner similar to **23** from lepidine and ethyl 5-methylpyridine-2-carboxylate (**22**). ^{1}H NMR (400 MHz, $CDCl_3$): δ 8.85 (d, J = 4.5 Hz, 1H), 8.59 (bs, 1H), 8.12 (d, J = 8.54 Hz, 1H), 8.01 (d, J = 8.03 Hz, 1H), 7.97 (ddd, J = 7.53, 7.53, 1.5 Hz, 1H), 7.70 (ddd, J = 7.03, 7.03, 1.5 Hz, 1H), 7.52 (ddd, J = 7.03, 7.03, 1.5 Hz, 1H), 7.66 (d, J = 8.03 Hz, 1H), 7.40 (d, J = 4.5 Hz, 1H), 5.01 (s, 2H), 2.45 (s, 3H). MS (ES) m/z 263 $(M + H)^+$.

2-(Quinolin-4-yl)-1-(1,3-thiazol-2-yl)ethanone (31). To an ice-cooled solution of 2-acetylthiazole (2.54 g, 20 mmol) in THF was added portionwise sodium hydride (60% oil suspension, 2.4 g, 60 mmol). The reaction mixture was stirred at 0 °C for 1 h and then heated to reflux for 2 h. After it was cooled at 0 °C, 4-chloroquinoline (3.26 g, 20 mmol) was added, and the reaction mixture was stirred at room temperature for 30 min and then heated to reflux for 2 days. After it was cooled, the reaction was quenched by addition of water and the solution was extracted with EtOAc. The organic phase was washed with water, dried over sodium sulfate, and evaporated. The crude product was purified by flash column chromatography on silica gel eluting with CH_2Cl_2/methanol 99/1 to afford **31** (0.5 g, 10%). ^{1}H NMR (300 MHz, $CDCl_3$): δ 8.80(d, J =

4.33 Hz, 1H), 8.08 (d, J = 8.48 Hz, 1H), 8.03 (d, J = 3.02 Hz, 1H), 7.99 (d, J = 8.48 Hz, 1H), 7.70 (d, J = 3.02 Hz, 1H), 7.66 (ddd, J = 6.97, 6.97, 1.32 Hz, 1H), 7.50 (ddd, J = 7.17, 6.97, 1.32 Hz, 1H), 7.38 (d, J = 4.33 Hz, 1H), 7.19 (s, 2H). GC-MS m/z 254.

2-(Naphthalen-1-yl)-1-(pyridin-2-yl)ethanone (32). To a supension of magnesium (2.5 g, 102.8 mmol) in anhydrous diethyl ether (20 mL), a solution of 1-(chloromethyl)naphthalene (20 g, 90.4 mmol) in anhydrous diethyl ether (80 mL) was added dropwise, under nitrogen atmosphere. The reaction mixture was heated to reflux for 20 min. The Grignard reagent was then added to a solution of ethyl picolinate (14.3 g, 94.6 mmol) in anhydrous diethyl ether (50 mL). After completion of the addition, diethyl ether was added (70 mL) and the reaction mixture was stirred at room temperature for 18 h. The mixture was quenched with a saturated aqueous ammonium chloride solution and extracted with CH_2Cl_2. The organic layer was dried over sodium sulfate and evaporated. The crude product was purified by flash column chromatography on silica gel eluting with CH_2Cl_2 to afford **32** (5 g, 22.4%). ^{1}H NMR (200 MHz, $CDCl_3$): δ 8.35 (bd, J = 4.58 Hz, 1H), 7.90−7.80 (m, 2H), 7.70−7.60 (m, 3H), 7.45−7.30 (m, 4H), 7.20−7.10 (m, 2H), reported as enol form (−O*H* not observed). GC-MS m/z 247.

2-Methyl[1,5]naphthyridine (36). A mixture of concentrated sulfuric acid (14 mL), sodium *m*-nitrobenzenesulfonate (11.30 g, 50 mmol), boric acid (1.55 g, 39 mmol), and iron sulfate heptahydrate (0.90 g, 3.23 mmol) was stirred at room temperature. Glycerol (8 mL) was added followed by 3-amino-6-picoline (**33**, 2.79 g, 25 mmol) and water (14 mL). The mixture was heated at 135 °C for 18 h. The reaction mixture was cooled to room temperature, basified using 4 N sodium hydroxide, and extracted with EtOAc. The organic extracts were combined and then preadsorbed onto silica gel (20 mL) prior to Biotage chromatography (using a 90 g silica gel cartridge) and eluting with EtOAc to afford **36** (2.01 g, 55%) as a light brown crystalline solid. ^{1}H NMR (400 MHz, $CDCl_3$): δ 8.92 (dd, J = 4.14, 1.51 Hz, 1H), 8.33 (d, J = 8.53 Hz, 1H), 8.29 (d, J = 8.53 Hz, 1H), 7.62 (dd, J = 8.53, 4.14 Hz, 1H), 7.54 (d, J = 8.53 Hz, 1H), 2.72 (s, 3H). MS (ES) m/z 145 (M + H)$^+$.

2,8-Dimethyl[1,5]naphthyridine (37). To an ice-cooled solution of 3-amino-4-methyl pyridine (**34**, 2.44 g, 0.023 mmol) in concentrated HCl (18 mL), acetaldehyde (3.58 g, 4.54 mL, 81.2 mmol) was added dropwise at 5 °C. The reaction mixture was stirred for 1 h at 0 °C and then was heated at reflux for 1 h. The dark brown suspension was allowed to cool to room temperature. Aqueous ammonia (18 mL) was added slowly with stirring, and a brown solid precipitated. This solid was filtered off and washed with water to give a crude solid, which was purified by flash column chromatography on silica gel, eluting with EtOAc and then chloroform/methanol/aqueous ammonia 60/10/1, to afford **37** (0.585 g, 16%). ^{1}H NMR (400 MHz, $CDCl_3$): δ 8.74 (d, J = 4.01 Hz, 1H), 8.22 (d, J = 9.04 Hz, 1H), 7.50 (d, J = 9.04 Hz, 1H), 7.44 (d, J = 4.01 Hz, 1H), 2.80 (s, 3H), 2.76 (s, 3H). MS (ES) m/z 159 (M + H)$^+$.

2-Methyl-6-chloro[1,5]naphthyridine (39). To an ice-cooled solution of 2-methoxy-5-aminopyridine (**35**, 7.86 g, 0.063 mmol) in concentrated HCl (50 mL), acetaldehyde (12.01 g, 15.2 mL, 0.27 mmol) was added dropwise at 0 °C. The reaction mixture was stirred for 1 h at 0 °C and then heated to reflux for 1 h. The black brown solid was filtered off, washed with water (3 × 100 mL), dried over sodium sulfate, and evaporated to give 2-hydroxy-6-methyl[1,5]naphthyridine (4.04 g, 36%) as a brown solid. This compound was used without purification in the next step. ^{1}H NMR (400 MHz, $CDCl_3$): δ 8.01 (dd, J = 9.54 Hz, 1H), 7.69 (d, J = 8.53 Hz, 1H), 7.32 (d, J = 8.53 Hz, 1H), 6.90 (d, J = 9.53 Hz, 1H), 2.65 (s, 3H). A suspension of 2-hydroxy-6-methyl[1,5]naphthyridine (**38**, 9.38 g, 58.55 mmol) in $POCl_3$ (85 mL) was heated to reflux for 1.5 h. The dark brown mixture was cooled to room temperature and was added dropwise to a stirred mixture of aqueous ammonia (0.88 M, 750 mL) and ice. The precipitate was filtered off, washed with water, and dried in vacuo at 50 °C to afford **39** as a brown solid (6.84 g, 65%). ^{1}H NMR (400 MHz, $CDCl_3$): δ 8.26 (d, J = 8.54 Hz, 1H), 8.20 (d, J = 9.04 Hz, 1H), 7.59 (d, J = 8.54 Hz, 1H), 7.54 (d, J = 9.04 Hz, 1H), 2.78 (s, 3H). MS (ES) m/z 179 (M + H)$^+$.

1-(Pyridin-2-yl)-2-([1,5]naphthyridin-2-yl)ethanone (41). A solution of **36** (1.03 g, 7.14 mmol) and ethyl picolinate (1.07 g, 7.14 mmol) in anhydrous THF (40 mL) was placed under a N_2 atmosphere and cooled with an ice bath to −78 °C. Potassium bis(trimethylsilyl) amide (0.5 M solution in toluene, 28.6 mL, 14.32 mmol) was added dropwise over 10 min. This mixture was stirred at −78 °C for 1 h and then warmed to room temperature for 20 h. Saturated aqueous ammonium chloride (100 mL) was added to the reaction mixture with stirring, and the mixture was partitioned between EtOAc and water. The aqueous phase was extracted with EtOAc. The organic layers were combined, washed with water, dried over sodium sulfate, and evaporated to give **41** as an orange yellow solid (1.78 g, quantitative). ^{1}H NMR (400 MHz, $CDCl_3$): δ 8.70−8.60 (m, 2H), 8.14 (d, J = 7.53 Hz, 1H), 7.98 (d, J = 9.53 Hz, 1H), 7.89 (bd, J = 9.04 Hz, 1H), 7.85 (dd, J = 8.03, 2.01 Hz, 1H), 7.50 (dd, J = 8.53, 4.01 Hz, 1H), 7.38 (m, 1H), 7.29 (d, J = 9.54 Hz, 1H), 6.93 (s, 1H), reported as enol form (−O*H* not observed). MS (APCI) m/z 250 (M + H)$^+$.

1-(6-Methyl-pyridin-2-yl)-2-([1,5]naphthyridin-2-yl)-ethanone (44). Compound **36** (4.34 g, 30.1 mmol) and methyl 6-methylpicolinate (5 g, 33.11 mmol) were coupled as described for **41** to afford **42** as an orange solid (6 g, 76%). ^{1}H NMR (300 MHz, $CDCl_3$): δ 8.98 (dd, J = 4.14, 1.51 Hz, 1H), 8.39 (d, J = 8.48 Hz, 2H), 8.10 (s, 1H), 7.87−7.81 (m, 2H), 7.66 (dd, J = 8.66, 8.28 Hz, 1H), 7.57 (dd, J = 7.92, 7.72 Hz, 1H), 7.15 (bd, J = 7.54 Hz, 1H), 2.60 (s, 3H), reported as the enol form (−O*H* not observed). MS (APCI) m/z 264 (M + H)$^+$.

1-(3-Chlorophenyl)-2-(1,5-naphthyridin-2-yl)ethanone (46). Compound **36** (3 g, 20.8 mmol) and ethyl 3-chlorobenzoate (3.84 g, 20.8 mmol) were coupled as described for **41** to afford **43** as a yellow solid (4.36 g, 74.3%); mp 119 °C. ^{1}H NMR (300 MHz, $CDCl_3$): δ 8.58 (dd, J = 4.52, 1.51 Hz, 1H), 7.90 (d, J = 9.42 Hz, 1H), 7.86−7.83 (m, 1H), 7.79 (d, J = 8.29 Hz, 1H), 7.74 (dt, J = 9.04, 1.51 Hz, 1H), 7.42 (dd, J = 4.52, 4.34 Hz, 1H), 7.38−7.27 (m, 2H), 7.10 (d, J = 9.04 Hz, 1H), 6.07 (s, 1H), reported as the enol form (−O*H* not observed). MS (APCI) m/z 283 (M + H)$^+$.

1-(Pyridin-2-yl)-2-(quinolin-4-yl)ethanone (47). 2-Methylquinoline (2.5 g, 17.5 mmol) and ethyl picolinate (2.64 g, 17.5 mmol) were coupled as described for **41** to afford **47** as orange bright crystals (3.18 g, 73%). ^{1}H NMR (250 MHz, $CDCl_3$): δ 15.75 (brs, 1H), 8.66 (d, J = 5.02 Hz, 1H), 8.17 (d, J = 8.03 Hz, 1H), 7.84 (td, J = 7.53, 1.51 Hz, 1H), 7.72 (d, J = 9.04 Hz, 1H), 7.60−7.50 (m, 3H), 7.37−7.26 (m, 2H), 7.00 (d, J = 9.54 Hz, 1H), 6.82 (s, 1H), reported as the enol form. MS (ES) m/z 249 (M + H)$^+$.

General Procedure for the Preparation of Aminothiazole Derivatives. 4-(Pyridin-2-yl)-5-(quinolin-4-yl)-1,3-thiazol-2-amine (1). To a solution of **23** (12.8 g, 51.67 mmol) in THF (50 mL) in a peptide vessel was added polymer-supported pyridinium perbromide (1 g/mmol of resin, 51.67 g), and the suspension was shaken overnight at room temperature. The resin was removed by filtration, with the filtrate being added directly to thiourea (1 equiv) as a solution in ethanol (80 mL). The resin was washed with ethanol (2 × 10 mL), and the filtrate was added to the reaction mixture. The mixture was heated to reflux for 4 h, allowed to cool at room temperature, and concentrated. The residue was dissolved in EtOAc and washed with aqueous sodium carbonate. The organic layer was dried over sodium sulfate, concentrated, and purified by flash column chromatography on silica gel eluting with CH_2Cl_2/methanol/Et_3N: 98/1/1. The solid obtained was recrystallized from 2-propanol to give **1** a pale yellow solid (8.2 g, 52%); mp 228 °C. ^{1}H NMR (300 MHz, $CDCl_3$): δ 8.73 (d, J = 4.52 Hz, 1H), 7.91 (d, J = 8.29 Hz, 1H), 7.80 (d, J = 4.71 Hz, 1H), 7.74 (d, J = 7.91 Hz, 1H), 7.68−7.53 (m, 3H), 7.37−7.28 (m, 2H), 7.26 (bs, 2H), 6.99−6.91 (m, 1H). MS (APCI) m/z 305 (M + H)$^+$. HR-MS: calcd for $C_{17}H_{12}N_4S$ (M + H), 305.0861;

found, 305.0839. Analytical HPLC $t_R = 1.64$ min, 100% pure (A), $t_R = 1.88$ min, 100% pure (B).

The following compounds were prepared using a similar procedure with appropriate ethanones.

4-(Pyridin-3-yl)-5-(quinolin-4-yl)-1,3-thiazol-2-amine (2). Compound **24** (0.52 g, 2.09 mmol) was reacted as described for **1**. The crude product was crystallized from EtOAc, to afford **2** as an orange solid (0.112 g, 17.6%); mp 232 °C. ^{1}H NMR (300 MHz, DMSO-d_6): δ 8.73 (d, $J = 4.33$ Hz, 1H), 8.24−8.21 (m, 1H), 8.14 (dd, $J = 4.71$, 1.51 Hz, 1H), 7.91 (bd, $J = 8.48$ Hz, 1H), 7.66−7.54 (m, 2H), 7.42−7.17 (m, 5H), 7.00 (dd, $J = 7.92$, 8.10 Hz, 1H). MS (ES) m/z 305 $(M + H)^+$. HR-MS: calcd for $C_{17}H_{12}N_4S$ (M + H), 305.0861; found, 305.0871. Analytical HPLC $t_R = 1.56$ min, 100% pure (A), $t_R = 1.85$ min, 100% pure (B).

5′-(Quinolin-4-yl)-2,4′-bi-1,3-thiazol-2′-amine (3). Compound **31** (0.254 g, 1 mmol) was reacted as described for **1** to afford **3** as yellow crystals (0.08 g, 26%); mp 238 °C. ^{1}H NMR (250 MHz, $CDCl_3$): δ 8.88 (d, $J = 4.33$ Hz, 1H), 8.04 (d, $J = 8.48$ Hz, 1H), 7.74 (d, $J = 7.92$ Hz, 1H), 7.69 (d, $J = 8.48$ Hz, 1H), 7.60−7.51 (4H, m), 7.47 (dd, $J = 7.91$, 7.15 Hz, 1H), 7.37 (d, $J = 3.20$ Hz, 1H). MS (APCI) m/z 311 $(M + H)^+$. HR-MS: calcd for $C_{15}H_{10}N_4S_2$ (M + H), 311.0425; found, 311.0399. Analytical HPLC $t_R = 1.69$ min, 100% pure (A), $t_R = 2.18$ min, 100% pure (B).

4-(2-Fluorophenyl)-5-(quinolin-4-yl)-1,3-thiazol-2-amine (4). Compound **25** (0.53 g, 2 mmol) was reacted as described for **1** to afford **4** as a yellow powder (0.14 g, 22%); mp 265−270 °C. ^{1}H NMR (250 MHz, DMSO-d_6): δ 8.87 (d, $J = 4.58$ Hz, 1H), 8.10 (d, $J = 8.24$ Hz, 1H), 8.02 (d, $J = 8.54$ Hz, 1H), 7.80 (dd, $J = 8.24$, 8.24 Hz, 1H), 7.66−7.48 (m, 4H), 7.37 (d, $J = 4.58$ Hz, 1H), 7.35−7.27 (m, 1H), 7.19 (dd, $J = 7.33$, 7.63 Hz 1H), 7.04 (dd, $J = 8.24$, 8.24 Hz, 1H). MS (APCI) m/z 322 $(M + H)^+$. HR-MS: calcd for $C_{18}H_{12}FN_3S$ (M + H), 322.0814; found, 322.0829. Analytical HPLC $t_R = 1.96$ min, 100% pure (A), $t_R = 2.14$ min, 100% pure (B).

4-[2-(Methoxy)phenyl]-5-(quinolin-4-yl)-1,3-thiazol-2-amine (5). Compound **26** (0.483 g, 1.7 mmol) was reacted as described for **1** to afford **5** as a pale yellow powder (0.04 g, 7%); mp 222−225 °C. ^{1}H NMR (300 MHz, $CDCl_3$): δ 8.65 (d, $J = 4.58$ Hz, 1H), 8.04 (d, $J = 8.54$ Hz, 1H), 7.97 (d, $J = 8.54$ Hz, 1H), 7.59 (dd, $J = 7.02$, 7.02 Hz, 1H), 7.40−7.27 (m, 2H), 7.11 (d, $J = 4.58$ Hz, 1H), 7.09−7.04 (m, 1H), 6.76 (dd, $J = 7.33$, 7.33 Hz, 1H), 6.52 (d, $J = 8.24$ Hz, 1H), 5.42 (bs, 2H), 2.99 (s, 3H). MS (APCI) m/z 334 $(M + H)^+$. HR-MS: calcd for $C_{19}H_{15}N_3OS$ (M + H), 334.1014; found, 334.0985. Analytical HPLC $t_R = 1.93$ min, 100% pure (A), $t_R = 2.10$ min, 100% pure (B).

4-(5-Chloro-pyridin-2-yl)-5-(quinolin-4-yl)-1,3-thiazol-2-amine (6). Compound **27** (0.296 g, 1.05 mmol) was reacted as described for **1** to afford **6** as a yellow solid (0.225 g, 63%). ^{1}H NMR (400 MHz, DMSO-d_6): δ 8.84 (d, $J = 4.02$ Hz, 1H), 8.02 (d, $J = 8.03$ Hz, 1H), 7.97−7.94 (m, 1H), 7.90−7.87 (m, 2H), 7.75−7.68 (m, 2H), 7.47−7.41 (m, 4H). MS (APCI) m/z 339 $(M + H)^+$. HR-MS: calcd for $C_{17}H_{11}ClN_4S$ (M + H), 339.0471; found, 339.0474. Analytical HPLC $t_R = 2.03$ min, 100% pure (A), $t_R = 2.17$ min, 100% pure (B).

4-(4-Chloro-pyridin-2-yl)-5-(quinolin-4-yl)-1,3-thiazol-2-amine (7). Compound **28** (0.25 g, 0.88 mmol) was reacted as described for **1** to afford **7** as brown crystals (0.14 g, 47%). ^{1}H NMR (400 MHz, DMSO-d_6): δ 8.86 (d, $J = 4.52$ Hz, 1H), 8.03 (d, $J = 8.53$ Hz, 1H), 7.94 (d, $J = 2$ Hz, 1H), 7.88 (d, $J = 5.52$ Hz, 1H), 7.75−7.68 (m, 2H), 7.50−7.44 (m, 4H), 7.22 (dd, $J = 5.52$, 2 Hz, 1H). MS (APCI) m/z 339 $(M + H)^+$. HR-MS: calcd for $C_{17}H_{11}ClN_4S$ (M + H), 339.0471; found, 339.0462. Analytical HPLC $t_R = 1.88$ min, 100% pure (A), $t_R = 2.17$ min, 100% pure (B).

4-(5-Methyl-pyridin-2-yl)-5-(quinolin-4-yl)-1,3-thiazol-2-amine (8). Compound **29** (0.3 g, 1.15 mmol) was reacted as described for **1** to afford **8** as a yellow solid (0.18 g, 49%). ^{1}H NMR (400 MHz, DMSO-d_6): δ 8.68 (d, $J = 4.52$ Hz, 1H), 7.87 (d, $J = 8.03$ Hz, 1H), 7.64−7.56 (m, 3H), 7.54 (dd, $J = 7.03$, 7.03 Hz, 1H), 7.40 (d, $J = 8.03$ Hz, 1H), 7.30−7.23 (m, 2H), 7.20 (bs, 2H), 2.07 (bs, 3H). MS (APCI) m/z 319 $(M + H)^+$. HR-MS: calcd for $C_{18}H_{14}N_4S$ (M + H), 319.1017; found, 319.0985. Analytical HPLC $t_R = 1.77$ min, 100% pure (A), $t_R = 1.99$ min, 100% pure (B).

5-(Naphthalen-1-yl)-4-(pyridin-2-yl)- 1,3-thiazol-2-amine (9). Compound **32** (0.4 g, 1.62 mmol) was reacted as described for **1** to afford **9** as a yellow solid (0.04 g, 8%); mp 179 °C. ^{1}H NMR (200 MHz, $CDCl_3$): δ 7.84 (bd, $J = 4.58$ Hz, 1H), 7.82−7.56 (m, 2H), 7.62−7.56 (m, 2H), 7.52 (dd, $J = 7.94$, 7.32 Hz, 1H), 7.28 (m, 3H), 7.13 (dd, $J = 4.89$, 4.89 Hz, 1H), 6.89 (dd, $J = 4.89$, 4.89 Hz, 1H), $-NH_2$ not observed. MS (APCI) m/z 304 $(M + H)^+$. HR-MS: calcd for $C_{18}H_{13}N_3S$ (M + H), 304.0908; found, 304.0926. Analytical HPLC $t_R = 2.33$min, 100% pure (B). Analytical HPLC $t_R = 7.71$min, 100% pure (C).

5-(1,8-Naphthyridin-4-yl)-4-(pyridin-2-yl)-1,3-thiazol-2-amine (10). A solution of 4-methyl[1,8]- naphthyridine (**21**, 0.38 g, 2.64 mmol) and ethyl picolinate (0.4 g, 2.64 mmol) in anhydrous THF (20 mL) was stirred under nitrogen and cooled to −78 °C. Potassium bis(trimethylsilyl)amide (0.5 M solution in toluene, 10.5 mL, 5.27 mmol) was added dropwise over 10 min. The reaction mixture was then stirred at −78 °C for 1 h and allowed to cool to room temperature for 18 h. Saturated aqueous ammonium chloride was added, and the mixture was partitioned between EtOAc and water. The aqueous phase was extracted with EtOAc. The organic layers were combined, washed with water, dried over sodium sulfate, and evaporated to give the 2-(1,8-naphthyridin-4-yl)-1-(2-pyridinyl)ethanone (**30**, 0.34 g, 0.56 mmol). Compound **30** was reacted immediately with bromine (0.035 mL, 0.68 mmol) in dioxane (10 mL) without further purification. The brown suspension was stirred at room temperature for 1 h and then evaporated to dryness. Thiourea (0.093 g, 1.45 mmol) and ethanol (10 mL) were added, and the mixture was heated at 78 °C for 3 h. The reaction mixture was cooled to room temperature and treated with aqueous ammonia (0.88, 10 mL). After evaporation to dryness, the crude product was purified by flash column chromatography on silica gel eluting with chloroform/methanol/aqueous ammonia 100/8/1 and crystallized from ethanol/diethyl ether to afford **10** as a brown solid (0.085 g, 50%). ^{1}H NMR (400 MHz, DMSO-d_6): δ 9.04 (d, $J = 4.5$ Hz, 1H), 8.99 (dd, $J = 7.53$, 3.52 Hz, 1H), 8.10 (d, $J = 8.03$ Hz, 1H), 7.91 (d, $J = 7.53$ Hz, 1H), 7.85 (d, $J = 3.52$ Hz, 1H), 7.80−7.72 (m, 1H), 7.56 (d, $J = 4$ Hz, 1H), 7.47 (bs, 2H), 7.41 (dd, $J = 7.53$, 3.52 Hz, 1H), 7.10−7.08 (m, 1H). MS (APCI) m/z 306 (MH+). HR-MS: calcd for $C_{16}H_{11}N_5S$ (M + H), 306.0813; found, 306.0795. Analytical HPLC $t_R = 1.11$ min, 100% pure (A), $t_R = 1.53$ min, 100% pure (B).

5-(1,5-Naphthyridin-2-yl)-4-(pyridin-2-yl)-1,3-thiazol-2-amine (11). A solution of **41** (6.63 g, 26.6 mmol) in dioxane (300 mL) was treated with bromine (1.65 mL, 31.9 mmol). The orange suspension was stirred at room temperature for 1 h and then concentrated. The residue was dissolved in ethanol (500 mL), thiourea (2.22 g, 2.93 mmol) was added, and the reaction mixture was heated at 78 °C for 4 h. The reaction was cooled to room temperature, and an aqueous solution of ammonia (0.88 M, 50 mL) was added with stirring. The mixture was evaporated, and the residue was dissolved in CH_2Cl_2 and washed with water (300 mL). The organic phase was extracted with 1 N hydrochloric acid (300 mL, 2 × 200 mL). The aqueous layers were basified with aqueous sodium hydroxide 35% (800 mL) and extracted with CH_2Cl_2. The organic phase was dried over sodium sulfate and evaporated to give the crude product as a brown powder. This powder was crystallized from acetonitrile to afford **11** (1.26 g, 16%) as yellow crystals; mp 114 °C. ^{1}H NMR (400 MHz, DMSO-d_6): δ 8.87 (dd, $J = 4.04$ Hz, 1.51, 1H,), 8.53 (bd, $J = 4.54$ Hz, 1H), 8.28 (bd, $J = 8.09$ Hz, 1H), 8.08 (d, $J = 9.10$ Hz, 1H), 7.94 (dd, $J = 7.58$, 1.51 Hz, 1H), 7.80 (bd, $J = 8.09$ Hz, 1H), 7.72 (dd, $J = 4.04$, 8.59 Hz, 1H), 7.56 (bs, 2H), 7.50 (d, $J = 8.59$ Hz, 1H), 7.44 (dd, $J = 5.06$, 6.67 Hz, 1H). MS (APCI) m/z 306 $(M + H)^+$. HR-MS: calcd for $C_{16}H_{11}N_5S$ (M + H), 306.0813; found, 306.0800. Analytical HPLC $t_R = 1.77$ min, 100% pure (A), $t_R = 1.78$ min, 100% pure (B).

4-(Pyridin-2-yl)- 5-(quinolin-2-yl)-1,3-thiazol-2-amine (12). Compound **47** (0.5 g, 2.02 mmol) was reacted as described

for **11** to afford **12** a yellow solid (0.17 g, 27.7%). ^{1}H NMR (400 MHz, DMSO-d_6): δ 8.68 (d, J = 4.02 Hz, 1H), 8.01 (d, J = 8.53 Hz, 1H), 7.87 (d, J = 8.53 Hz, 1H), 7.75−7.64 (m, 4H), 7.47 (dd, J = 7.03, 7.03 Hz, 1H), 7.35−7.27 (m, 2H), 5.20 (bs, 2H). MS (APCI) m/z 305 $(M + H)^+$. HR-MS: calcd for $C_{17}H_{12}N_4S$ (M + H), 305.0861; found, 305.0858. Analytical HPLC t_R = 1.96 min, 100% pure (A), t_R = 2.12 min, 100% pure (B).

5-[6-(Ethoxy)-1,5-naphthyridin-2-yl]-4-(pyridin-2-yl)-1,3-thiazol-2-amine (13). To a solution of **39** (3 g, 18.72 mmol) and ethyl picolinate (1.93 mL, 18.72 mmmol) in anhydrous THF (100 mL) under a N_2 atmosphere at −78 °C, potassium bis(trimethylsilyl)amide (0.5 M solution in toluene, 75 mL, 37.44 mmol) was added dropwise over 10 min. This mixture was stirred at −78 °C for 1 h and then at room temperature for 18 h. The reaction mixture was quenched by adding saturated aqueous ammonium chloride and partitioned between EtOAc and water. The aqueous phase was extracted with EtOAc. The organic layers were combined, washed with water, dried over sodium sulfate, and evaporated to give 6-chloro[1,5]naphthyridin-2-yl)-1-(pyridin-2-yl)ethanone (**42**, 0.34 g, 1.19 mmol), which was treated without purification with bromine (0.074 mL, 1.44 mmol) in dioxane (20 mL). The resulting brown suspension was stirred at room temperature for 1 h and then evaporated to dryness. Thiourea (0.099 g, 1.31 mmol) and ethanol (10 mL) were added, and the mixture was heated at 78 °C for 2 h. The reaction mixture was allowed to cool at room temperature and treated with aqueous ammonia (0.88M, 2 mL). After evaporation to dryness, the crude product was purified by flash column chromatography on silica gel eluting with EtOAc/cyclohexane 1/1 to afford **13** an orange red solid (0.04 g, 9.6%). ^{1}H NMR (400 MHz, DMSO-d_6): δ 8.50 (d, J = 4 Hz, 1H), 8.13 (d, J = 9.04 Hz, 1H), 7.91 (dd, J = 8.03, 1.50 Hz, 1H), 7.84 (d, J = 9.04 Hz, 1H), 7.77 (bd, J = 8.03 Hz, 1H), 7.45 (d, J = 9.04 Hz, 1H), 7.43−7.38 (m, 3H), 7.18 (d, J = 9.04 Hz, 1H), 4.44 (q, J = 7.03 Hz, 2H), 1.38 (t, J = 7.03 Hz, 3H). MS (APCI) m/z 350 $(M + H)^+$. HR-MS: calcd for $C_{18}H_{15}N_5OS$ (M + H), 350.1075; found, 350.1065. Analytical HPLC t_R = 2.78 min, 98.2% pure (A), t_R = 2.30 min, 98.4% pure (B).

5-(8-Methyl-1,5-naphthyridin-2-yl)-4-(pyridin-2-yl)-1,3-thiazol-2-amine (14a). Compound **37** (0.585 g, 3.7 mmol) and ethyl picolinate (0.559 g, 3.7 mmol) were coupled as described for **13** to give a mixture of 2-(6-methyl-1,5-naphthyridin-4-yl)-1-(2-pyridinyl)ethanone and 2-(8-methyl-1,5-naphthyridin-2-yl)-1-(2-pyridinyl)ethanone (**43**), which was used in the next step without purification. This mixture (0.132 g, 0.501 mmol) was reacted as described for **11** and the resulting two isomers were separated by chromatography on silica gel eluting with EtOAc to afford **14a** as a yellow solid (0.095 g, 60%). ^{1}H NMR (400 MHz, $CDCl_3$): δ 8.85 (1H, d, J = 4.52 Hz), 8.66 (m, 1H), 8.21 (d, J = 9.04 Hz, 1H), 8.11 (m, 1H), 7.94 (m, 1H), 7.76 (d, J = 4.52 Hz, 1H), 7.70 (d, J = 9.04 Hz, 1H), 7.63 (m, 1H), 2.50 (s, 3H). MS (APCI) m/z 320 (MH+). HR-MS: calcd for $C_{17}H_{13}N_5S$ (M + H), 320.0970; found, 320.0939. Analytical HPLC t_R = 1.72 min, 100% pure (A), t_R = 1.94 min, 100% pure (B).

The isomer 5-(6-methyl-1,5-naphthyridin-4-yl)-4-(pyridin-2-yl)-1,3-thiazol-2-amine (**14b**) was also identified. ^{1}H NMR (400 MHz, $CDCl_3$): δ 8.70 (d, J = 4.77 Hz, 1H), 8.28 (d, J = 8.54 Hz, 1H), 8.14 (m, 1H); 7.89 (dd, J = 7.7,7.7 Hz 1H), 7.72(d, J = 7.78 Hz, 1H), 7.65 (d, J = 8.53 Hz, 1H), 7.38(d, J = 4.77 Hz, 1H), 7.33(m, 1H), 2.54 (s, 3H). MS (APCI) m/z 320 (MH+). HR-MS: calcd for $C_{17}H_{13}N_5S$ (M + H), 320.0970; found, 320.0985. Analytical HPLC t_R = 2.10 min, 100% pure (A), t_R = 1.72 min, 100% pure (B).

4-(6-Methyl-pyridin-2-yl)-5-(1,5-naphthyridin-2-yl)-1,3-thiazol-2-amine (15). Compound **44** (0.131 g, 0.5 mmol) was reacted as described for **11** to afford **15** as yellow crystals (0.027 g, 17%); mp 188 °C. ^{1}H NMR (300 MHz, $CDCl_3$): δ 8.78 (dd, J = 4.14, 1.51 Hz, 1H), 8.20 (bd, J = 8.48 Hz, 1H), 7.97 (d, J = 8.86 Hz, 1H), 7.65−7.42 (m, 3H), 7.37 (d, J = 7.73 Hz, 1H), 7.11 (d, J = 7.73 Hz, 1H), 5.32 (s, 2H), 2.49 (s, 3H). MS (APCI) m/z 320 $(M + H)^+$. HR-MS: calcd for $C_{17}H_{13}N_5S$ (M + H), 320.0970; found, 320.0954. Analytical HPLC t_R = 1.59 min, 100% pure (A), t_R = 1.85 min, 100% pure (B).

4-(4-Fluorophenyl)-5-(1,5-naphthyridin-2-yl)-1,3-thiazol-2-amine (16). Compound **42** (0.60 g, 4.16 mmol) and ethyl 4-fluorobenzoate (0.84 g, 4.99 mmol) were coupled as described for **13** to give 1-(4-fluorophenyl)-2-(1,5-naphthyridin-2-yl)-ethanone **45** as a mixture with the enol form. MS (APCI) m/z: 267 $(M + H)^+$. This mixture (0.87 g, 3.27 mmol) was treated as described for **1** to afford **16**, after recrystallization from 2-propanol, as a yellow solid (0.35 g, 34.7%); mp 213 °C. ^{1}H NMR (300 MHz, DMSO-d_6): δ 8.88 (dd, J = 4.14, 1.51 Hz, 1H), 8.28 (d, J = 7.91 Hz, 1H), 8.12 (d, J = 9.04 Hz, 1H), 7.75 (dd, J = 4.14, 4.14 Hz, 1H), 7.66−7.55 (m, 4H), 7.39−7.24 (m, 3H). MS (APCI) m/z 323 $(M + H)^+$. HR-MS: calcd for $C_{17}H_{11}FN_4S$ (M + H), 323.0766; found, 323.0757. Analytical HPLC t_R = 1.91 min, 98.7% pure (A), t_R = 2.12 min, 98.6% pure (B).

4-(4-Chlorophenyl)-5-(1,5-naphthyridin-2-yl)-1,3-thiazol-2-amine (17). Compound **46** (4.36 g, 15.43 mmol) was reacted as described for **12** to afford **17**, after recrystallization from EtOAc, as a yellow solid (3.25 g, 62.2%); mp 219−220 °C. ^{1}H NMR (400 MHz, DMSO-d_6): δ 8.86 (dd, J = 4.04, 1.01 Hz, 1H), 8.26 (d, J = 8.59 Hz, 1H), 8.12 (d, J = 8.59 Hz, 1H), 7.73 (dd, J = 4.04, 4.04 Hz, 1H), 7.60 (bd, J = 5.56 Hz, 2H), 7.54−7.43 (m, 2H), 7.34 (d, J = 9.09 Hz, 1H), $-NH_2$ not observed. MS (APCI) m/z 339 $(M + H)^+$. HR-MS: calcd for $C_{17}H_{11}ClN_4S$ (M + H), 339.0471; found, 339.0500. Analytical HPLC t_R = 2.09 min, 100% pure (A), t_R = 2.30 min, 100% pure (B).

2-[3-(Pyridin-2-yl)-1*H*-pyrazol-4-yl]-1,5-naphthyridine (18). To a solution of **41** (0.39 g, 1.56 mmol) in anhydrous DMF (6 mL) were added acetic acid (0.32 mL, 5.61 mmol) and DMF·DMA (0.62 mL, 4.68 mmol). The reaction mixture was stirred for 1 h at room temperature, next hydrazine monohydrate (1.7 mL, 35 mmol) was added, and the mixture was heated at 50 °C for 2 h. The cooled reaction mixture was poured into water and extracted with EtOAc. The organic layer was washed with saturated aqueous $NaHCO_3$, dried over sodium sulfate, and concentrated in a vacuum. The crude solid was recrystallized from acetonitrile to afford **18** as an off-white solid (0.31 g, 73%). ^{1}H NMR (400 MHz, DMSO-d_6): δ 13.59 (bs, 1H), 8.93 (dd, J = 4.04, 1.51 Hz, 1H), 8.57 (bs, 1H), 8.34−8.25 (m, 3H), 7.94−7.81 (m, 3H), 7.75 (dd, J = 8.50, 4.04 Hz, 1H), 7.44−7.38 (m, 1H). MS (ES) m/z 274 $(M + H)^+$. HR-MS: calcd for $C_{16}H_{11}N_5$ (M + H), 274.1093; found, 274.1103. Analytical HPLC t_R = 1.28 min, 100% pure (A), t_R = 1.69 min, 100% pure (B).

2-[3-(6-Methyl-pyridin-2-yl)-1*H*-pyrazol-4-yl]-1,5-naphthyridine (19). Compound **44** (0.6 g, 2.28 mmol) was treated as described for **18** to afford **19** as a yellow solid (0.2 g, 30.6%); mp 191 °C. ^{1}H NMR (300 MHz, $CDCl_3$): δ 11.57 (bs, 1H), 8.78 (dd, J = 4.14, 1.70 Hz, 1H), 8.20 (d, J = 8.78 Hz, 2H), 7.91 (s, 1H), 7.67 (d, J = 8.67 Hz, 2H), 7.47 (dd, J = 8.48, 4.14 Hz, 1H), 7.42−7.33 (m, 1H), 6.97 (d, J = 7.72 Hz, 1H), 2.40 (s, 3H). MS (APCI) m/z 288 $(M + H)^+$. HR-MS: calcd for $C_{17}H_{13}N_5$ (M + H), 288.1249; found, 288.1226. Analytical HPLC t_R = 1.50min, 100% pure (A), t_R = 1.76 min, 98.9% pure (B).

Molecular Modeling. The docking experiments were performed using GOLD V1.1[22] in TGF-β−FKBP12 complex. A single hydrogen bond constraint was added during calculations, guiding the quinoline N1 or naphthyridine N5 to interact with the protein backbone NH of His-283. The parameters were maintained as standard default GOLD V1.1 settings with the following exceptions. The floodfill radius, defining the active site search center, was increased to 12 Å. This radius was measured from a dummy atom located at the centroid generated from the heavy atom positions of five key residues: Lys-232, Leu-260, Ser-280, His-283, and Asp-351. Ten poses per ligand docking were saved, and the top scoring pose was taken to be the favored pose in the majority of cases. Only in the event of an obvious failure was the top pose discarded and an alternative, lower scoring pose selected. To ensure that a range of solutions was available for scrutiny, early termination was disabled. Visualization was performed with Sybyl 6.x (Tripos) and Insight II (Accelrys).

X-ray Crystallography: Crystallization of the Complex of Human ALK5 with Inhibitor 19. The kinase domain of ALK5 was expressed as a glutathione S-transferase (GST) fusion protein in baculovirus-infected sf9 cells. After purification on glutathione Sepharose, GST was removed by thrombin cleavage and ALK5 was further purified on an ATP-Sepharose affinity column. The purified protein was concentrated to 9 mg/mL in the presence of inhibitor and was in a solution containing 50 mM tris, pH 8.0, 8% glycerol, ~200 mM NaCl, 1.5 mM EDTA, and 2 mM DTT. Crystals of ALK5 complexed with inhibitor compound **19** grew as a clump of needles in 3 weeks at 4 °C using the vapor diffusion method and a reservoir containing 20% PEG 4000, 0.1 M Tris HCl, pH 8.5, and 0.2 M magnesium chloride. The crystals of the complex are orthorhombic, space group $P2_12_12_1$, with cell constants $a = 42.07$ Å, $b = 77.78$ Å, and $c = 89.59$ Å. The structure was determined by molecular replacement with a model consisting of coordinates for all protein atoms from residues 201 to 500 of human ALK5 from the published structure of the cytoplasmic domain of type I TGF-β receptor in complex with FKBP12 (PDB code 1B6C). The structure was refined at 2.0 Å resolution. The final values for R_{cryst} and R_{free} were 0.224 and 0.275. The coordinates have been deposited in the Protein Data Bank, accession number 1VJY.

ALK5 Fluorescence Polarization Binding Assay. Fluorescence polarization is a method that is well-documented in the literature.[23] Kinase inhibitor compounds, conjugated to fluorophores, can be used as fluorescent ligands to monitor ATP competitive binding of other compounds to a given kinase. The increase in depolarization of plane polarized light, caused by release of the bound ligand into solution, is measured as a polarization/anisotropy value. Compound binding to ALK5 was tested on purified recombinant GST−ALK5 (residues 198−503). Displacement of rhodamine green fluorescently labeled ATP competitive inhibitor[24] by different concentrations of test compounds was used to calculate a binding pIC_{50}. GST−ALK5 was added to a buffer containing 62.5 mM Hepes, pH 7.5, 1 mM DTT, 12.5 mM $MgCl_2$, 1.25 mM CHAPS (all reagents obtained from Sigma), and 1 nM rhodamine green-labeled ligand so that the final ALK5 concentration was 10 nM based on active site titration of the enzyme. Forty microliters of the enzyme/ligand reagent was added to 384 well assay plates containing 1 μL of different concentrations of test compound. The plates were read immediately on a LJL Acquest fluorescence reader (Molecular Devices) with excitation, emission, and dichroic filters of 485, 530, and 505 nm, respectively. The fluorescence polarization for each well was calculated by the Acquest and was then imported into curve fitting software for construction of concentration−response curves.

ALK5 Autophosphorylation Assay. The kinase domain of ALK5 (Franzen, P. 1993) (amino acids 162−503) was cloned by PCR and expressed in a baculovirus/Sf9 cells system. The protein was 6-His tagged in the C terminus and purified by affinity chromatography using a Ni^{2+} column, and the obtained material was used to assess compound activity in an autophosphorylation assay. Purified enzyme (10 nM) was incubated in 50 μL of Tris buffer (Tris 50 mM, pH 7.4; NaCl, 100 mM; $MgCl_2$, 5 mM; $MnCl_2$, 5 mM; and DTT, 10 mM). The enzyme was preincubated with different concentrations of compounds (0.1% DMSO final concentration in the test) for 10 min at 37 °C. The reaction was then initiated by the addition of 3 μM ATP (0.5 μCi γ-33P-ATP). After 15 min at 37 °C, phosphorylation was stopped by the addition of SDS−PAGE sample buffer (50 mM Tris-HCl, pH 6.9, 2.5% glycerol, 1% SDS, and 5% β-mercaptoethanol). The samples were boiled for 5 min at 95 °C and run on a 12% SDS−PAGE. Dried gels were exposed to a phosphor screen overnight. ALK5 autophosphorylation was quantified using a Storm imaging system (Molecular Dynamics).

Cellular Assays to Measure Anti-TGF-β Activity of ALK5 Inhibitors. The activity of compounds was tested in a transcriptional assay in HepG2 cells. The cells were stably transfected with a PAI-1 promoter driving a luciferase (firefly) reporter gene.[25] The stably transfected cells responded to TGF-β stimulation by a 10−20-fold increase in luciferase activity as compared to control conditions.

To test anti-TGF-β activity of compounds, the cells were seeded in 96 well microplates at a concentration of 35000 cells per well in 200 μL of serum-containing medium. The microplates were then placed for 24 h in a cell incubator at 37 °C, 5% CO_2 atm. The compounds dissolved in DMSO were then added at concentrations of 50 nM to 10 μM (final concentration of DMSO 1%) for 30 min prior to the addition of recombinant TGF-β (1 ng/mL) (R&D systems). After an overnight incubation, the cells were washed with PBS and lysed by addition of 10 μL of passive lysis buffer (Promega). Inhibition of luciferase activity relative to control groups was used as a measure of compound activity. A concentration−response curve was constructed from which an IC_{50} value was determined graphically.

Acknowledgment. We acknowledge Dr. Andrew Brewster for discussions and comments on the manuscript. Special thanks are given to Ruth Lehr for the expression and purification of the protein, to the GSK kinase enzymology group for setting up and running the kinases assays, to Florence Loriolle for running the HTS, and to Cécile Bertho-Ruault for her assistance in mass spectra.

Supporting Information Available: Structure of the rhodamine green-labeled ligand used for the binding assay. This material is available free of charge via the Internet at http://pubs.acs.org.

References

(1) Massague, J.; Blain, S. W.; Lo, R. S. TGF β Signaling in Growth Control, Cancer, and Heritable Disorders. *Cell* **2000**, *103*, 295−309.
(2) Border, W. A.; Noble, N. A. Transforming Growth Factor β in Tissue Fibrosis. *N. Engl. J. Med.* **1994**, *331*, 1286−1292.
(3) Blobe, G. C.; Schiemann, W. P.; Lodish, H. F. Role of Transforming Growth Factor β in Human Disease. *N. Engl. J. Med.* **2000**, *342*, 1350−1358.
(4) Anscher, M. S.; Peters, W. P.; Reisenbichler, H.; Petros, W. P.; Jirtle, R. L. Transforming Growth Factor β as a Predictor of Liver and Lung Fibrosis after Autologous Bone Marrow Transplantation for Advanced Breast Cancer. *N. Engl. J. Med.* **1993**, *328*, 1592−1598.
(5) Akhurst, R. J.; Derynck, R. TGF-β Signaling in Cancer−A Double-Edged Sword. *Trends Cell Biol.* **2001**, *11*, S44−S51.
(6) Kingsley, D. M. The TGF-β Superfamily: New Members, New Receptors, and New Genetic Tests of Function in Different Organisms. *Genes Dev.* **1994**, *8*, 133−146.
(7) Attisano, L.; Wrana, J. L. Signal Transduction by the TGF-β Superfamily. *Science* **2002**, *296*, 1646−1647.
(8) Miyazano, K. TGF-β Receptors and Signal Transduction. *Int. J. Hematol.* **1997**, *65*, 97−104.
(9) Huse, M.; Chen, Y. G.; Massagué, J.; Kuriyan, J. Crystal Structure of the Cytoplasmic Domain of the Type I TGF β Receptor in Complex with FKBP12. *Cell* **1999**, *96*, 425−436.
(10) Derynck, R.; Zhang, Y.; Feng, X.-H. Transcriptional Activators of TGF-β Responses: Smads. *Cell* **1998**, *95*, 737−740.
(11) Gallagher, T. F.; Seibel, G. L.; Kassis, S.; Laydon, J. T.; Blumenthal, M. J.; Lee, J. C.; Lee, D.; Boehm, J. C.; Fier-Thompson, S. M.; Abt, J. W.; Soreson, M. E.; Smietana, J. M.; Hall, R. F.; Garigipati, R. S.; Bender, P. E.; Erhard, K. F.; Krog, A. J.; Hofmann, G. A.; Sheldrake, P. L.; McDonnell, P. C.; Kumar, K. F.; Young, P. R.; Adams, J. A. Regulation of Stress-Induced Cytokine Production by Pyridinylimidazoles; Inhibition of CSBP Kinase. *Bioorg. Med. Chem.* **1997**, *5*, 49−64.
(12) Lee, J. C.; Kassis, S.; Badger, A.; Adams, J. L. p38 Mitogen-Activated Protein Kinase Inhibitors−Mechanisms and Therapeutic Potentials. *Pharmacol. Ther.* **1999**, *82*, 389−397.
(13) Eyers, P. A.; Craxton, M.; Morrice, N.; Cohen, P.; Goedert, M. Conversion of SB-203580-Insensitive MAP Kinase Family Members to Drug-Sensitive Forms to a Single Amino-Acid Substitution. *Chem. Biol.* **1998**, *5*, 321−328.
(14) Gellibert, F. J.; Mathews, N. Pyridinyl-Substituted Pyrazole Derivatives Useful against TGF-β Overexpression, and Their Preparation and Use. *PCT Int. Appl.* **2002**, WO 2002066462 A1.
(15) Sawyer, J. S.; Anderson, B. D.; Beight, D. W.; Campbell, R. M.; Jones, M. L.; Herron, D. K.; Lampe, J. W.; McCowan, J. R.; McMillen, W. T.; Mort, N.; Parsons, S.; Smith, E. C. R.; Vieth,

M.; Weir, L. C.; Yan, L.; Zhang, F.; Yingling, J. M. Synthesis and Activity of New Aryl- and Heteroaryl-Substituted Pyrazole Inhibitors of the Transforming Growth Factor-β Type I Receptor Kinase Domain. *J. Med. Chem.* **2003**, *46*, 3953−3956.

(16) Singh, J.; Chuaqui, C. E.; Boriack-Sjodin, P. A.; Lee, W.-C.; Pontz, T.; Corbley, M. J.; Cheung, H.-K.; Arduini, R. M.; Mead, J. N.; Newman, M. N.; Papadatos, J. L.; Bowes, S.; Josiah, S.; Ling, L. E. Successful Shape-Based Virtual Screening: The Discovery of a Potent Inhibitor of the Type I TGF.β. Receptor Kinase (TβRI). *Bioorg. Med. Chem. Lett.* **2003**, *13*, 4355−4359.

(17) Chambers, R. J.; Marfat, A. Regiospecific Carboalkoxylation of 2,5-Dibromopyridine. *Synth. Commun.* **1997**, *27*, 515−520.

(18) Paudler, W. W.; Kress, T. J. A One Step Synthesis of 1,8-Naphthyridines. *J. Org. Chem.* **1967**, *32*, 832−833.

(19) Armarego, W. L. F. Naphthyridines. III. Tetrahydro- and Decahydro-1,5-,-1,6-,-1,7-, and -1,8-naphthyridines. *J. Chem. Soc. C* **1967**, 377−383.

(20) Najiba, D.; Carpentier, J.-F.; Castanet, Y.; Biot, C.; Brocard, J.; Mortreux, A. Palladium-Catalysed Carbonylations of Dichloroquinoline or Simple Dichloropyridines. *Tetrahedron Lett.* **1999**, *40*, 3719−3722.

(21) Gudmundsson, K. S.; Hinkley, J. M.; Brieger, M. S.; Drach, J. C.; Townsend, L. B. An Improved Large-Scale Synthesis of 2-Amino-4-chloropyridine and Its Use for the Convenient Preparation of Various Polychlorinated 2-Aminopyridines. *Synth. Commun.* **1997**, *27*, 861−870.

(22) Jones, G.; Willett, P.; Glen, R. C.; Leach, A. R.; Taylor, R. Development and Validation of a Genetic Algorithm for Flexible Docking. *J. Mol. Biol.* **1997**, *267*, 727−748.

(23) (a) Pope, A. J.; Haupts, U. M.; Moore, K. J. Homogeneous Fluorescence Readouts for Miniaturized High-Throughput Screening: Theory and Practice. *Drug Discovery Today* **1999**, *4* (8), 350−362. (b) Owicki, J. C. Fluorescence Polarization and Anisotropy in High Throughput Screening: Perspectives and Primer. *J. Biomol. Screening* **2000**, *5* (5), 297−306. (c) Hubert, C. L.; Sherling, S. E.; Johnston, P. A.; Stancato, L. F. Data Concordance from a Comparison between Filter Binding and Fluorescence Polarization Assay Formats for Identification of ROCK-II Inhibitors. *J. Biomol. Screening* **2003**, *8* (4), 399−409. (d) Lynch, B. A.; Loiacono, K. A.; Tiong, C. L.; Adams, S. E.; MacNeil, I. A. A Fluorescence Polarization Based Src-SH2 Binding Assay. *Anal. Biochem.* **1997**, *247*, 77−82.

(24) The fluorescent ligand is described in the following patent application: Patent WO02/24680, 2000. The structure of the ligand is described in the Supporting Information.

(25) Dennler, S.; Itoh, S.; Vivien, D.; ten Dijke, P.; Huet, S.; Gauthier, J. M. Direct Binding of Smad3 and Smad4 to Critical TGF-B Inducible Elements in the Promoter of Human Plasminogen Activator Inhibitor-Type1 Gene. *EMBO J.* **1998**, *17*, 3091−3100.

JM0400247